

PhD Thesis

Physical Layer Security in Frequency-Domain Time-Reversal SISO OFDM Communication

Sidney Golstein

Promotor:

Pr. Dr. Ir. Julien Sarrazin

Co-promotor:

Pr. Dr. Ir. Philippe De Doncker

September 8, 2020

Contents

Acronyms	4
1 Introduction	1
2 Handshake Protocol	2
3 Communication Protocol	2
3.1 Conventional FD TR SISO OFDM Communication	2
3.1.1 Received sequence at the intended position	4
3.1.2 Received sequence at the unintended position	4
3.2 FD TR SISO OFDM communication with AN addition	4
3.2.1 AN Design	5
3.2.2 Received sequence at the intended position	6
3.2.3 Received sequence at the unintended position	6
4 Performance Assessment	7
4.1 SINR determination	7
4.1.1 At Bob, i.e., the intended position	7
4.1.2 At Eve, i.e., the unintended position	8
4.2 Optimal amount of AN to inject	11
4.2.1 Eve's estimator: same structure as Bob	11
4.2.2 Eve's estimator: matched filtering	11
4.3 Secrecy rate optimization via waterfilling	12
5 Simulation Results	13
5.1 Decoding results	13
5.2 Secrecy results	14
5.2.1 Comparaison between models and simulations	14
5.2.2 Comparison between the different decoding structures	15
5.2.3 Waterfilling Optimization	16
6 Conclusion & Perspectives	16
References	18
Appendices	19
A SINR derivation	19
A.1 At the intended position	19
A.2 At the unintended position	20
A.2.1 Eve and Bob with identical capacities	20
A.2.2 Matched Filtering	21
A.2.3 AN suppression	26
A.2.4 LMMSE	28

B	Optimal amount of AN to inject derivation	29
B.1	Despreading at Eve	29
B.2	Matched filtering at Eve	29
C	Momentum computation of complex-valued random normal variables	30
C.1	Real-valued random normal variable	30
C.2	Complex-valued random normal variable	30

List of Figures

1	Security scenario	2
2	Conventional FD TR SISO OFDM system	2
3	Illustration of conventional FD TR SISO OFDM system	3
4	FD TR SISO OFDM system with added artificial noise	5
5	Illustration of FD TR SISO OFDM system with added artificial noise	5
6	Matched filtering decoding structure	9
7	AN killer decoding structure	10
8	BER as a function of the level of noise for different AN energy values, back-off rate (BOR) = 4	13
9	BER as a function of AN energy for different BOR values, $E_b/N_0 = 15\text{dB}$	13
10	Secrecy Rate curves, analytic vs simulation for the 2 models, $E_b/N_0 = 25\text{ dB}$, BOR = 4	14
11	Optimal amount of AN to inject, Bob and Eve with the same decoding structure, $E_b/N_0 = 5\text{ dB}$	14
12	Secrecy Rate curves for the different decoding structures at Eve, $E_b/N_0 = 25\text{ dB}$, BOR = 4	15
13	SR optimization via waterfilling, Bob and Eve with same capabilities, $E_b/N_0 = 20\text{ dB}$	16
A.1	CDF of the inverse chi-square distribution of $\nu = 2$ degrees of freedom.	28

Acronyms

AN	artificial noise
AWGN	additive white Gaussian noise
BER	bit-error-rate
BOR	back-off rate
CDF	cumulative distribution function
CFR	channel frequency response
CSI	channel state information
FD	frequency-domain
i.i.d.	identically and independently distributed
IoT	Internet-Of-Things
LMMSE	linear minimum mean square error
MIMO	multiple-input multiple-output
MMSE	minimum mean square error
MSE	mean square error
OFDM	orthogonal frequency-division multiplexing
PAPR	peak-to-average-power ratio
PDF	probability density function
PLS	physical layer security
RV	random variable
SINR	signal-to-interference-plus-noise ratio
SISO	single-input single-output
SNR	signal-to-noise ratio
SR	secrecy rate
SVD	singular value decomposition
TD	time-domain
TR	time-reversal
USRP	Universal Software Radio Peripheral
ZF	zero-forcing

1 Introduction

Due to their broadcast nature, wireless communications remain unsecured. With the deployment of 5G as an heterogeneous network possibly involving different radio access technologies, physical layer security (PLS) has gained recent interests in order to secure wireless communications, [1, 2, 3]. PLS classically takes benefit of the characteristics of wireless channels, such as multipath fading, to improve security of communications against potential eavesdroppers. A secure communication can exist as soon as the eavesdropper channel is degraded with respect to the legitimate user one, [4]. This can be achieved by increasing the signal-to-interference-plus-noise ratio (SINR) at the intended position and decreasing the SINR at the unintended position if its channel state information (CSI) is known, and/or, by adding an artificial noise (AN) signal that lies in the null space of the legitimate receiver's channel. While many works implement these schemes using multiple antennas at the transmitter, only few ones intend to do so with single-input single-output (SISO) systems [5, 6, 7, 8].

In [5], a technique is proposed that combines a symbol waveform optimisation in time-domain (TD) to reach a desired SINR at the legitimate receiver and an AN injection using the remaining available power at the transmitter when eavesdropper's CSI is not known. Another approach to increase the SINR in SISO systems is time-reversal (TR). This has the advantage to be implemented with a simple precoder at the transmitter. TR achieves a gain at the intended receiver position only, thereby naturally offering a possibility of secure communication, [9]. TR is achieved by up/downsampling the signal in the TD. It has been shown in [10] that TR can be equivalently achieved in frequency-domain (FD) by replicating and shifting the signal spectrum. FD implementation has the advantage to be easily performed using orthogonal frequency-division multiplexing (OFDM). To further enhance the secrecy, few works combine TD TR precoding with AN injection [6, 7, 8]. In these works, the AN is added either on all the channel taps or on a set of selected taps. While the condition for AN generation is given, its derivation is however not detailed. Furthermore, the impact of BOR, defined as the up/downsampling rate [11], has not been yet studied in the literature.

An approach to establish secure communication using a FD TR precoder in SISO OFDM systems is proposed. An AN signal is designed to maximize the secrecy rate (SR) of the communication in presence of a passive eavesdropper whose CSI is supposed unknown. The proposed scheme uses only frequency diversity inherently present in multipath environments to achieve security. It can therefore be used in SISO systems and is then well-suited for resource-limited nodes such as encountered in Internet-Of-Things (IoT) for instance. Indeed, multiple-input multiple-output (MIMO) capabilities require several antennas and as many transceivers and ADC/DAC, which might not fit into small-size sensors and could be too power-consuming for such IoT scenarios. Furthermore, the OFDM implementation makes this approach compatible with LTE and 5G systems.

Notation: the italic lower-case letter denotes a complex number. Greek letter corresponds to a scalar, the bold lower-case letter denotes a column vector. Bold upper-case letter corresponds to a matrix; \mathbf{I}_N is $N \times N$ identity matrix; $(\cdot)^{-1}$, $(\cdot)^*$, $(\cdot)^H$ are respectively the inverse, the complex conjugate and the Hermitian transpose operators; $\mathbb{E}[\cdot]$ is the expectation operator; $|\cdot|$ is the modulus operator (element-wise modulus if we deal with a matrix); \odot is the element-wise (hadamard) product between two vectors of same dimension.

2 Handshake Protocol

Prior to the secure data transmission between Alice and Bob, a handshake protocol must take place. Depending on it, Eve will obtain different knowledges about the communication parameters which will lead to different decoding capabilities and so, different security performances.

3 Communication Protocol

A scheme of the secure FD TR SISO OFDM communication is presented in Fig.1 where Alice transmits wireless data to a legitimate receiver Bob. An eavesdropper (Eve) tries to eavesdrop the data. We assume that Alice does not have any information about Eve's CSI and perfectly knows Bob's instantaneous CSI.

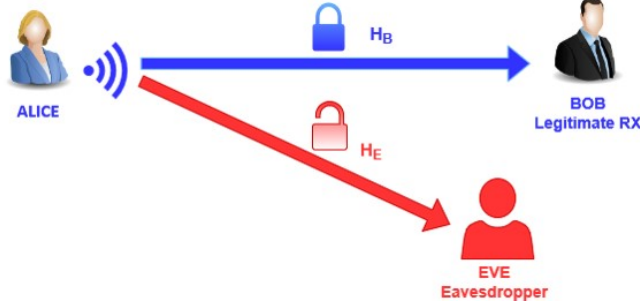


Figure 1: Security scenario

3.1 Conventional FD TR SISO OFDM Communication

The FD TR precoding scheme is illustrated in Fig.2. The communication is designed such that the data focuses at the legitimate receiver's position.

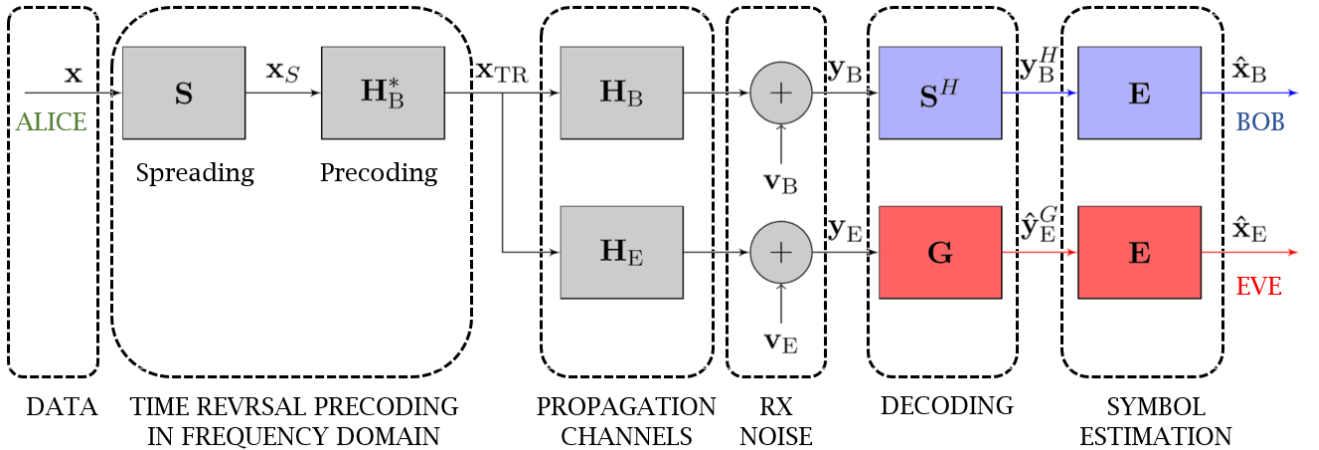


Figure 2: Conventional FD TR SISO OFDM system

The data is conveyed onto OFDM symbols with Q subcarriers. Without loss of generality, we consider that only one OFDM block \mathbf{x} is sent over the FD TR precoding SISO OFDM system. A data block \mathbf{x} is composed of N symbols x_n (for $n = 0, \dots, N-1$, with $N \leq Q$). The symbol x_n is assumed to be a zero-mean random variable (RV) with variance $\mathbb{E}[|x_n|^2] = \sigma_x^2 = 1$ (i.e., a normalized constellation is considered). The data block \mathbf{x} is then spread with a factor $U = Q/N$, called BOR, via the matrix \mathbf{S} of

size $Q \times N$. The matrix \mathbf{S} is called the spreading matrix and stacks U times $N \times N$ diagonal matrices, with diagonal elements taken from the set $\{\pm 1\}$ and being identically and independently distributed (i.i.d.) in order not to increase the peak-to-average-power ratio (PAPR) as suggested in [12]. This matrix is normalized by a factor \sqrt{U} in order to have $\mathbf{S}^H \mathbf{S} = \mathbf{I}_N$:

$$\mathbf{S} = \frac{1}{\sqrt{U}} \cdot \begin{pmatrix} \pm 1 & 0 & \dots & 0 \\ 0 & \pm 1 & \dots & 0 \\ \vdots & & \ddots & \vdots \\ 0 & 0 & \dots & \pm 1 \\ & \vdots & \vdots & \\ \pm 1 & 0 & \dots & 0 \\ 0 & \pm 1 & \dots & 0 \\ \vdots & & \ddots & \vdots \\ 0 & 0 & \dots & \pm 1 \end{pmatrix} ; \quad [Q \times N] \quad (1)$$

As stated in [10], the idea behind the spreading is that up-sampling a signal in the TD is equivalent to the repetition and shifting of its spectrum in the FD. In doing so, each data symbol will be transmitted onto U different subcarriers with a spacing of N subcarriers, introducing frequency diversity. The spread sequence is then precoded before being transmitted. This requires the knowledge of Bob channel frequency response (CFR) at Alice. We consider that Alice can perfectly estimate Bob CFR. The channels between Alice and Bob (\mathbf{H}_B) and between Alice and Eve (\mathbf{H}_E) are assumed to be static during the transmission of one OFDM symbol. \mathbf{H}_B and \mathbf{H}_E are $Q \times Q$ diagonal matrices whose elements are $h_{B,q}$ and $h_{E,q}$ (for $q = 0, \dots, Q-1$) and follow a zero-mean unit-variance complex normal distribution, i.e., their modulus follow a Rayleigh distribution. We also consider that the overall channel energies are normalized to unity for each channel realization. The precoding matrix \mathbf{H}_B^* is also a diagonal matrix with elements $h_{B,q}^*$. At the receiver, a despreading operation is performed by applying \mathbf{S}^H . We consider that Bob knows the spreading sequence and apply a zero-forcing (ZF) equalization. In the following, different decoding structures \mathbf{G} will be investigated at Eve. These different schemes will lead to different level of security performances. A perfect synchronization is also assumed at Bob and Eve positions.

An illustration of such a communication is presented in Fig.3 where a block of $N = 4$ symbols is spread by a factor $U = 4$ and then sent via $Q = 16$ subcarriers. We observe that, at Bob, the received sequence is perfectly recovered which is not the case at Eve's position.

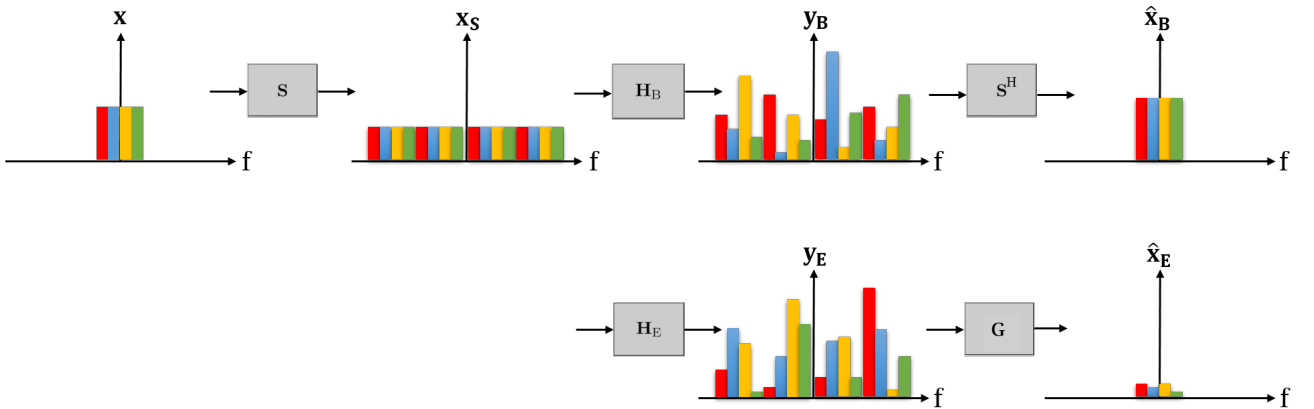


Figure 3: Illustration of conventional FD TR SISO OFDM system

3.1.1 Received sequence at the intended position

After despreading, the received sequence at Bob is:

$$\mathbf{y}_B^H = \mathbf{S}^H |\mathbf{H}_B|^2 \mathbf{S} \mathbf{x} + \mathbf{S}^H \mathbf{v}_B \quad (2)$$

where \mathbf{v}_B is the FD complex additive white Gaussian noise (AWGN). The noise's auto-correlation is $\mathbb{E}[|v_{B,n}|^2] = \sigma_{V,B}^2$ and the covariance matrix is $\mathbb{E}[(\mathbf{S}^H \mathbf{v}_B)(\mathbf{S}^H \mathbf{v}_B)^H] = \sigma_{V,B}^2 \mathbf{I}_N$. We also assume that the data symbol x_n and noise $v_{B,n}$ are independent of each other. In (2), each transmitted symbol is affected by a real gain at the position of the legitimate receiver since the product $\mathbf{H}_B \mathbf{H}_B^*$ is a real diagonal matrix. The gains differ between each symbol in the OFDM block but increases with an increase of the BOR value as each symbol would be sent on more subcarriers and would benefit from a larger frequency diversity gain. If we consider a fixed bandwidth, the TR focusing effect is enhanced for higher BOR's at the expense of the data rate. After ZF equalization, we obtain:

$$\hat{\mathbf{x}}_B = (\mathbf{S}^H |\mathbf{H}_B|^2 \mathbf{S})^{-1} (\mathbf{S}^H |\mathbf{H}_B|^2 \mathbf{S} \mathbf{x} + \mathbf{S}^H \mathbf{v}_B) = \mathbf{x} + (\mathbf{S}^H |\mathbf{H}_B|^2 \mathbf{S})^{-1} \mathbf{S}^H \mathbf{v}_B \quad (3)$$

From (3), we observe that the transmit data is perfectly recovered at high signal-to-noise ratio (SNR).

3.1.2 Received sequence at the unintended position

The data received at the unintended position is given by:

$$\mathbf{y}_E^G = \mathbf{G} \mathbf{H}_E \mathbf{H}_B^* \mathbf{S} \mathbf{x} + \mathbf{v}_E \quad (4)$$

where \mathbf{G} is a $N \times N$ filter matrix performed by Eve, \mathbf{v}_E is the complex AWGN. The noise auto-correlation is $\mathbb{E}[|v_{E,n}|^2] = \sigma_{V,E}^2$ and the covariance matrix is $\mathbb{E}[(\mathbf{S}^H \mathbf{v}_E)(\mathbf{S}^H \mathbf{v}_E)^H] = \sigma_{V,E}^2 \mathbf{I}_N$. In (4), $\mathbf{H}_E \mathbf{H}_B^*$ is a complex diagonal matrix. Therefore, due to the precoding, i.e., since the data transmission is designed to reach Bob position, each received symbol component will be affected by a random complex coefficient. The magnitude of this coefficient does not depend on the BOR value. It results in an absence of TR gain at the unintended position. As a consequence, worse decoding performance is obtained compared to the intended position. Eve needs lower noise power than Bob to reach the same bit-error-rate (BER). After ZF equalization, one obtains:

$$\hat{\mathbf{x}}_E = (\mathbf{G} \mathbf{H}_E \mathbf{H}_B^* \mathbf{S})^{-1} (\mathbf{G} \mathbf{H}_E \mathbf{H}_B^* \mathbf{S} \mathbf{x} + \mathbf{v}_E) = \mathbf{x} + (\mathbf{G} \mathbf{H}_E \mathbf{H}_B^* \mathbf{S})^{-1} \mathbf{G} \mathbf{v}_E \quad (5)$$

Equation (5) shows that in the classical FD TR SISO OFDM communication scheme, the data could potentially be recovered at Eve's position. A similar BER could be obtained at Eve if she is closer to Alice than Bob is and/or if its noise power is less than Bob's one. This motivates the addition of AN in order to corrupt the data detection at any unintended positions in order to secure the communication. In Section 4, different filtering structures \mathbf{G} will be investigated leading to different security performances of the scheme.

3.2 FD TR SISO OFDM communication with AN addition

In order to secure the communication between Alice and Bob, an AN signal \mathbf{w} is added after precoding to the useful signal \mathbf{x}_S at the transmitter side, as depicted in Fig. 4. The AN should not have any impact at Bob's position but should be seen as interference everywhere else since Alice does not have any information about Eve's CSI. Furthermore, this signal should not be guessed at the unintended

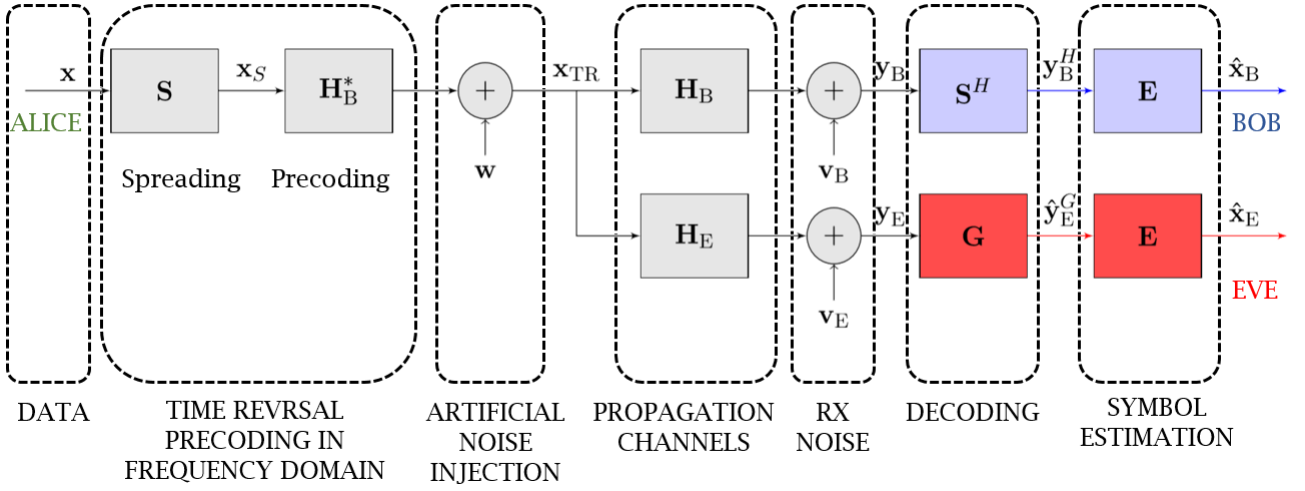


Figure 4: FD TR SISO OFDM system with added artificial noise

positions to ensure the secure communication. With these considerations, the transmitted sequence becomes:

$$\mathbf{x}_{\text{TR}} = \sqrt{\alpha} \mathbf{H}_B^* \mathbf{S} \mathbf{x} + \sqrt{1 - \alpha} \mathbf{w} \quad (6)$$

where $\alpha \in [0, 1]$ defines the ratio of the total power dedicated to the useful signal, knowing that $\mathbb{E} [|\mathbf{H}_B^* \mathbf{S} \mathbf{x}|^2] = \mathbb{E} [|\mathbf{w}|^2] = 1/U$. Whatever the value of α , the total transmitted power remains constant.

Fig.5 illustrates a scheme with additive AN. We sent a block of $N = 4$ symbols which is spread by a factor $U = 4$, i.e., the data is conveyed onto $Q = 16$ subcarriers. A block of 16 AN symbols is added (in pink). At bob's position, there is no influence of these AN symbols and the data is perfectly recovered. At Eve, the received symbols are corrupted by the AN signal and by the data precoding.

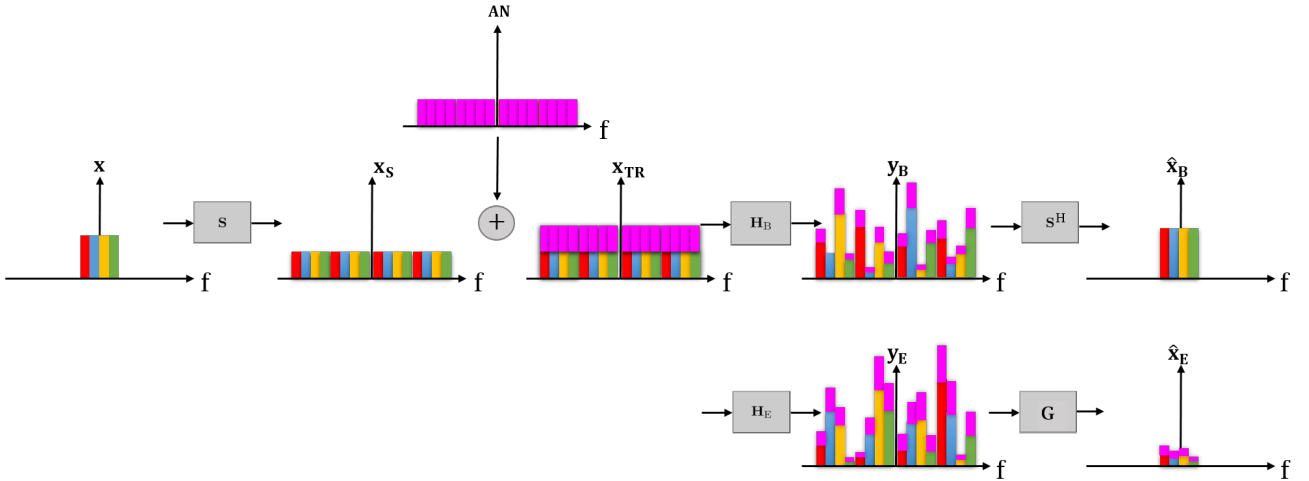


Figure 5: Illustration of FD TR SISO OFDM system with added artificial noise

3.2.1 AN Design

In order not to have any impact at the intended position, the AN signal must satisfy the following condition:

$$\mathbf{A} \mathbf{w} = \mathbf{0} \quad (7)$$

where $\mathbf{A} = \mathbf{S}^H \mathbf{H}_B \in \mathbb{C}^{N \times Q}$. Condition (7) ensures that \mathbf{w} lies in the right null space of \mathbf{A} . If we perform a singular value decomposition (SVD) of \mathbf{A} , we obtain:

$$\mathbf{A} = \mathbf{U} \left(\Sigma \mathbf{0}_{Q-N \times Q} \right) \begin{pmatrix} \mathbf{V}_1^H \\ \mathbf{V}_2^H \end{pmatrix} \quad (8)$$

where $\mathbf{U} \in \mathbb{C}^{N \times N}$ contains left singular vectors, $\Sigma \in \mathbb{C}^{N \times N}$ is a diagonal matrix containing singular values, $\mathbf{V}_1 \in \mathbb{C}^{Q \times N}$ contains right singular vectors associated to non-zero singular values, and $\mathbf{V}_2 \in \mathbb{C}^{Q \times Q-N}$ contains right singular vectors that span the right null space of \mathbf{A} . Therefore, the AN signal can be expressed as:

$$\mathbf{w} = \beta \mathbf{V}_2 \tilde{\mathbf{w}} \quad (9)$$

which ensures that (7) is satisfied for any arbitrary vector $\tilde{\mathbf{w}} \in \mathbb{C}^{Q-N \times 1}$. Since $Q = NU$, as soon as $U \geq 2$, there is a set of infinite possibilities to generate $\tilde{\mathbf{w}}$ and therefore the AN signal. In the following, we assume that $\tilde{\mathbf{w}}$ is a zero-mean circularly symmetric white complex Gaussian noise with covariance matrix $\mathbb{E} [\tilde{\mathbf{w}}(\tilde{\mathbf{w}})^H] = \mathbf{I}_{Q-N \times 1}$. The AN signal is then generated thanks to (9) and finally weighted by β to have an energy of $1/U$.

3.2.2 Received sequence at the intended position

After despreading, the received sequence at Bob is:

$$\mathbf{y}_B^H = \sqrt{\alpha} \mathbf{S}^H |\mathbf{H}_B|^2 \mathbf{S} \mathbf{x} + \mathbf{S}^H \mathbf{v}_B \quad (10)$$

Again, each transmitted symbol is affected by a real gain depending on the BOR value and weighted by $\sqrt{\alpha}$. One can observe that no AN contribution is present in (10) since (7) are respected. A ZF equalization is performed at the receiver leading to:

$$\hat{\mathbf{x}}_B = \left(\sqrt{\alpha} \mathbf{S}^H |\mathbf{H}_B|^2 \mathbf{S} \right)^{-1} \left(\sqrt{\alpha} \mathbf{S}^H |\mathbf{H}_B|^2 \mathbf{S} \mathbf{x} + \mathbf{S}^H \mathbf{v}_B \right) = \mathbf{x} + \left(\sqrt{\alpha} \mathbf{S}^H |\mathbf{H}_B|^2 \mathbf{S} \right)^{-1} \mathbf{S}^H \mathbf{v}_B \quad (11)$$

From (11), a perfect data recovery is possible in high SNR scenario.

3.2.3 Received sequence at the unintended position

The received sequence at the eavesdropper position has the form:

$$\mathbf{y}_E^G = \sqrt{\alpha} \mathbf{G} \mathbf{H}_E \mathbf{H}_B^* \mathbf{S} \mathbf{x} + \sqrt{1-\alpha} \mathbf{G} \mathbf{H}_E \mathbf{w} + \mathbf{G} \mathbf{v}_E \quad (12)$$

In (12), a term depending on the AN signal appears since $\mathbf{G} \mathbf{H}_E \mathbf{w} \neq \mathbf{0}$. This term introduces an interference at Eve and thus scrambles the received constellation even in a noiseless environment. After ZF equalization, the estimated symbols are:

$$\begin{aligned} \hat{\mathbf{x}}_E &= (\mathbf{G} \mathbf{H}_E \mathbf{H}_B^* \mathbf{S})^{-1} \left(\sqrt{\alpha} \mathbf{G} \mathbf{H}_E \mathbf{H}_B^* \mathbf{S} \mathbf{x} + \sqrt{1-\alpha} \mathbf{G} \mathbf{H}_E \mathbf{w} + \mathbf{G} \mathbf{v}_E \right) \\ &= \sqrt{\alpha} \mathbf{x} + \sqrt{1-\alpha} (\mathbf{G} \mathbf{H}_E \mathbf{H}_B^* \mathbf{S})^{-1} \mathbf{G} \mathbf{H}_E \mathbf{w} + (\mathbf{G} \mathbf{H}_E \mathbf{H}_B^* \mathbf{S})^{-1} \mathbf{G} \mathbf{v}_E \end{aligned} \quad (13)$$

Equation (13) shows that the addition of AN in the FD TR SISO OFDM communication can secure the data transmission. It is to be noted that, since \mathbf{w} is generated from an infinite set of possibilities, even if Eve knows its equivalent channel $\mathbf{H}_E \mathbf{H}_B^*$ and the spreading sequence, she cannot estimate the AN signal to try retrieving the data. The degree of security will depend on the amount of AN energy that is injected into the communication and on the decoding capabilities of Eve, as shown in Section 4.

4 Performance Assessment

The secrecy rate (SR) is defined as the maximum transmission rate that can be supported by the legitimate receiver's channel while ensuring the impossibility for the eavesdropper to retrieve the data, [13]. In the ergodic sense, it can be expressed as:

$$\begin{aligned} C_S &= \mathbb{E} [\log_2 (1 + \gamma_B) - \log_2 (1 + \gamma_E)] \quad , \quad \gamma_B > \gamma_E \\ &\leq \log_2 (1 + \mathbb{E} [\gamma_B]) - \log_2 (1 + \mathbb{E} [\gamma_E]) \end{aligned} \quad (14)$$

with γ_B and γ_E being respectively the SINR at Bob and Eve's positions. The inequality in (14) arises from the Jensen's inequality.

In the following, we consider these assumptions:

- Q subcarriers, back off rate = U , $N = Q/U$ symbols sent per OFDM block
- $\mathbf{H}_B = \mathbf{H}_{B,x} + j\mathbf{H}_{B,y} \sim \mathcal{CN}(0, 1) \sim \mathcal{N}(0, \frac{1}{2}) + j\mathcal{N}(0, \frac{1}{2})$
- $\mathbf{H}_E = \mathbf{H}_{E,x} + j\mathbf{H}_{E,y} \sim \mathcal{CN}(0, 1) \sim \mathcal{N}(0, \frac{1}{2}) + j\mathcal{N}(0, \frac{1}{2})$
- $h_{B,i} \perp h_{B,j}, \forall i \neq j$, i.e., no frequency correlation between Bob's channel subcarriers
- $h_{E,i} \perp h_{E,j}, \forall i \neq j$, i.e., no frequency correlation between Eve's channel subcarriers¹.
- $h_{B,i} \perp h_{E,j}, \forall i, j$, i.e., Bob and Eve are sufficiently spaced inducing no spatial correlation between their channels.

4.1 SINR determination

4.1.1 At Bob, i.e., the intended position

At Bob, the received signal after despreading is given by (10). Using the Jensen's inequality, a lower bound on the average SINR can be derived for the transmitted symbols n as:

$$\begin{aligned} \mathbb{E} [\gamma_{B,n}] &= \mathbb{E} \left[\frac{\alpha |k_n x_n|^2}{|v_{B,n}|^2} \right] = \alpha \mathbb{E} [|k_n x_n|^2] \mathbb{E} \left[\frac{1}{|v_{B,n}|^2} \right] \\ &\geq \frac{\alpha \mathbb{E} [|k_n x_n|^2]}{\mathbb{E} [|v_{B,n}|^2]} = \frac{\alpha \mathbb{E} [|k_n|^2] \mathbb{E} [|x_n|^2]}{\mathbb{E} [|v_{B,n}|^2]} \end{aligned} \quad (15)$$

where $k_n = \frac{1}{U} \sum_{i=0}^{U-1} |h_{B,n+iN}|^2$, x_n is the n^{th} data symbol, and $v_{B,n} = \frac{1}{\sqrt{U}} \sum_{i=0}^{U-1} |v_{B,n+iN}|$ is the n^{th} noise symbol component and where it is observed that $k_n \perp x_n \perp v_{B,n}$. We find²:

$$\begin{aligned} \mathbb{E} [|k_n|^2] &= \frac{\alpha(U+1)}{U} \\ \mathbb{E} [|x_n|^2] &= 1 \\ \mathbb{E} [|v_{B,n}|^2] &= \sigma_{V,B}^2 \end{aligned} \quad (16)$$

The SINR for a particular symbol at the intended position is then given by:

$$\mathbb{E} [\gamma_{B,n}] \geq \frac{\alpha (U+1)}{U \sigma_{V,B}^2} \quad (17)$$

¹Thanks to the design of the spreading matrix, the U subcarriers composing one symbol are spaced by $N = Q/U$ subcarriers. If this distance is larger than the coherence bandwidth of the channel, the assumption holds. This usually occurs in rich multipath environments and for sufficiently large bandwidths and moderate BOR values.

²See Appendix A

It was observed in simulations than the lower-bound (17) is tight enough to be used as an approximation of the averaged SINR at the intended position.

4.1.2 At Eve, i.e., the unintended position

At the unintended position, the received signal before ZF equalization is given by (12). Let's introduce $\mathbf{A}_1 = \sqrt{\alpha} \mathbf{G} \mathbf{H}_E \mathbf{H}_B^* \mathbf{S} \mathbf{x}$, $\mathbf{A}_2 = \mathbf{G} \mathbf{v}_E$ and $\mathbf{A}_3 = \sqrt{1-\alpha} \mathbf{G} \mathbf{H}_E \mathbf{w}$ being respectively the data component, the noise component and the AN component of the received signal for a particular decoding structure \mathbf{G} . Using the Jensen's inequality, an approximation of a lower-bound of the averaged SINR of the symbols n at the unintended position can be derived as³:

$$\begin{aligned} \mathbb{E} [\gamma_{E,n}] &= \mathbb{E} \left[\frac{|A_{1,n}|^2}{|A_{2,n} + A_{3,n}|^2} \right] \approx \mathbb{E} [|A_{1,n}|^2] \mathbb{E} \left[\frac{1}{|A_{2,n} + A_{3,n}|^2} \right] \\ &\geq \frac{\mathbb{E} [|A_{1,n}|^2]}{\mathbb{E} [|A_{2,n} + A_{3,n}|^2]} = \frac{\mathbb{E} [|A_{1,n}|^2]}{\mathbb{E} [|A_{2,n}|^2] + \mathbb{E} [|A_{3,n}|^2]} \end{aligned} \quad (18)$$

where $A_{1,n}$, $A_{2,n}$ and $A_{3,n}$ being respectively the data, noise and AN n^{th} symbol components of the received signal. The expression of the SINR at Eve will depend on her receiving structure \mathbf{G} and we will investigate four of them.

4.1.2.1 Same structure as Bob

In this scenario, Eve has the same capabilities as Bob, i.e., she despread the received signal thanks to $\mathbf{G} = \mathbf{S}^H$. In that case, the received signal is:

$$\mathbf{y}_E^G = \sqrt{\alpha} \mathbf{S}^H \mathbf{H}_E \mathbf{H}_B^* \mathbf{S} \mathbf{x} + \sqrt{1-\alpha} \mathbf{S}^H \mathbf{H}_E \mathbf{w} + \mathbf{S}^H \mathbf{v}_E \quad (19)$$

We then have

$$\begin{aligned} A_{1,n} &= \sqrt{\alpha} \frac{1}{U} \sum_{i=0}^{U-1} h_{E,n+iN} h_{B,n+iN}^* \\ A_{2,n} &= \frac{1}{\sqrt{U}} \sum_{i=0}^{U-1} v_{E,n+iN} \\ A_{3,n} &= \sqrt{1-\alpha} \frac{1}{\sqrt{U}} \sum_{i=0}^{U-1} h_{E,n+iN} w_{n+iN} \end{aligned} \quad (20)$$

After some mathematical manipulations, we have⁴:

$$\begin{aligned} \mathbb{E} [|A_{1,n}|^2] &= \frac{\alpha}{U} \\ \mathbb{E} [|A_{2,n}|^2] &= \sigma_{V,E}^2 \\ \mathbb{E} [|A_{3,n}|^2] &= (1-\alpha) \sigma_{AN}^2 \end{aligned} \quad (21)$$

which lead to an ergodic SINR at the unintended position given by:

$$\mathbb{E} [\gamma_{E,n}] \gtrapprox \frac{\alpha}{U(\sigma_{V,E}^2 + (1-\alpha) \sigma_{AN}^2)} \quad (22)$$

³Neglecting the covariance between $|A_{1,n}|^2$ and $|A_{2,n} + A_{3,n}|^2$, as done in the first line of (18), makes the nature of the bound, i.e., lower or upper, obtained for $\mathbb{E} [\gamma_{E,n}]$ uncertain. However, we have observed by simulations that it remains a lower one for all considered scenarios.

⁴see Appendix A

Low performances at Eve are expected with this decoding structure since the despreading operation will not coherently add the received symbol components. It is therefore suboptimal leading to high SR values. This will be confirmed in section 5.2.1.

4.1.2.2 Eve's estimator: matched Filtering

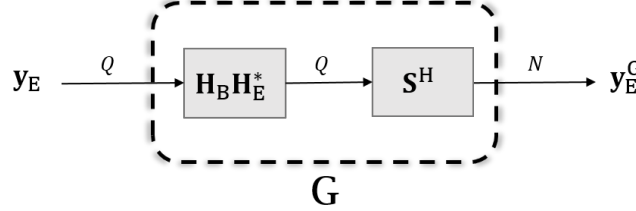


Figure 6: Matched filtering decoding structure

Eve can also perform a matched filtering to maximize its SNR before despreading. If we denote by $\Gamma_E = \mathbf{H}_E \mathbf{H}_B^* \mathbf{S}$, the decoding matrix is then given by: $\mathbf{G} = \Gamma_E^H$. It simply consists in performing a weight multiplication at each subcarrier and then perform despreading as shown in fig.6. This operation is possible since Eve can estimate $\mathbf{H}_E \mathbf{H}_B^*$ while receiving data from Alice. However, it requires more processing resources than the classical receiver of Bob since a processing is performed on the whole bandwidth, i.e., all Q subcarriers. This will lead to more efficient decoding performances at the eavesdropper. The received signal is then:

$$\mathbf{y}_E^G = \sqrt{\alpha} \mathbf{S}^H |\mathbf{H}_E|^2 |\mathbf{H}_B|^2 \mathbf{S} \mathbf{x} + \sqrt{1-\alpha} \mathbf{S}^H \mathbf{H}_B |\mathbf{H}_E|^2 \mathbf{w} + \mathbf{S}^H \mathbf{H}_E^* \mathbf{H}_B \mathbf{v}_E \quad (23)$$

If we compare the received signal at Bob (10) with the received signal at Eve (23), we remark that the data component in (23) will be more amplified than in (10). In fact, we amplify the data by a factor $\frac{U+3}{U}$ in (23), and only by a factor $\frac{U+1}{U}$ in (10)⁵. However, we note that the AN component of the received signal will be amplified with the matched filtering decoding strategy. With this structure, we have:

$$\begin{aligned} A_{1,n} &= \sqrt{\alpha} \frac{1}{U} \sum_{i=0}^{U-1} |h_{E,n+iN}|^2 |h_{B,n+iN}|^2 \\ A_{2,n} &= \frac{1}{\sqrt{U}} \sum_{i=0}^{U-1} h_{E,n+iN}^* h_{B,n+iN} v_{E,n+iN} \\ A_{3,n} &= \sqrt{1-\alpha} \frac{1}{\sqrt{U}} \sum_{i=0}^{U-1} h_{B,n+iN} |h_{E,n+iN}|^2 w_{n+iN} \end{aligned} \quad (24)$$

After computations, the expected values are:

$$\begin{aligned} \mathbb{E} [A_{1,n}^2] &= \alpha \frac{U+3}{U} \\ \mathbb{E} [A_{2,n}^2] &= \sigma_{V,E}^2 \\ \mathbb{E} [A_{3,n}^2] &= \frac{1-\alpha}{U+1} \end{aligned} \quad (25)$$

The details can be found in Appendix A. We then obtain an ergodic SINR which takes the following form:

$$\mathbb{E} [\gamma_{E,n}] \gtrsim \frac{\alpha \frac{U+3}{U}}{\sigma_{V,E}^2 + \frac{1-\alpha}{U+1}} \quad (26)$$

⁵see Appendix A

4.1.2.3 Eve's estimator: AN killer

Eve can adapt her decoder to kill the AN signal. In fact, by performing $\mathbf{G} = \mathbf{S}^H \mathbf{H}_B \mathbf{H}_E^{-1}$, the AN term will become $\sqrt{1-\alpha} \mathbf{S}^H \mathbf{H}_B \mathbf{H}_E^{-1} \mathbf{H}_E \mathbf{w} = \sqrt{1-\alpha} \mathbf{S}^H \mathbf{H}_B \mathbf{w} = \mathbf{0}$ since it is projected in the null space of $\mathbf{S}^H \mathbf{H}_B$. However, this considers that Eve is able to estimate its own channel \mathbf{H}_E , which is a very strong assumption. If Alice always communicates to Bob using \mathbf{H}_B^* as a precoder, the data received by Eve is always affected by a term $\mathbf{H}_B^* \mathbf{H}_E$ which avoids Eve to estimate \mathbf{H}_E with classical preamble-based channel estimation methods for instance. However, if an uncoded reference signal is sent by Alice at some point, the Eve might be able to estimate \mathbf{H}_E (if the channel remains constant between the time at which Alice sends a reference signal and at which Alice sends the \mathbf{H}_B^* -precoded data). It also requires a processing on the full bandwidth, as suggested in fig.7.

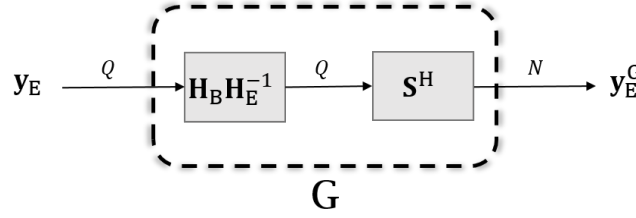


Figure 7: AN killer decoding structure

In that case, the received signal is:

$$\mathbf{y}_E^G = \sqrt{\alpha} \mathbf{S}^H |\mathbf{H}_B|^2 \mathbf{S} \mathbf{x} + \mathbf{S}^H \mathbf{H}_E^{-1} \mathbf{H}_B \mathbf{v}_E \quad (27)$$

The received signal (27) is similar to Bob's one (10) except that the noise term is multiplied by \mathbf{H}_E^{-1} which is not optimal. In fact, if \mathbf{H}_E has low gains at some subcarriers, the noise will be highly amplified. In that situation, we obtain:

$$\begin{aligned} A_{1,n} &= \sqrt{\alpha} \frac{1}{U} \sum_{i=0}^{U-1} |h_{B,n+iN}|^2 \\ A_{2,n} &= \frac{1}{\sqrt{U}} \sum_{i=0}^{U-1} h_{E,n+iN}^{-1} h_{B,n+iN} v_{E,n+iN} \end{aligned} \quad (28)$$

No analytic expression can be found for the expected value of the energy of the noise $\mathbb{E}[|A_{2,n}|^2]$ since we have to deal with $\frac{1}{|h_{E,n+iN}|^2}$ which follows an inverse chi-square distribution of $\nu = 2$ degrees of freedom. It therefore has an infinite mean⁶. Only the cumulative distribution function (CDF) of the noise energy can be derived, and consequently the CDF of the SINR for that decoding structure.

For the data symbol, we have:

$$\mathbb{E}[|A_{1,n}|^2] = \alpha \frac{U+1}{U} \quad (29)$$

The derivations are found in Appendix A.

4.1.2.4 Eve's estimator: LMMSE

The linear minimum mean square error (LMMSE) equalizer aims to minimize the mean square error (MSE) of the estimated symbol $\hat{\mathbf{x}}_E = \mathbf{G} \mathbf{y}_E^G$. The equalizer \mathbf{G} has to fulfill the orthogonality principle

⁶Intuitively, if one subcarrier has zero gain, which arises from example when two waves arrive with destructive interference, $\frac{1}{|h_{E,n+iN}|^2}$ will tend to infinity. This is why $\mathbb{E}[|A_{2,n}|^2] = +\infty$.

which states that the estimator $\hat{\mathbf{x}}_E$ achieves minimum mean square error (MMSE) if and only if:

$$\mathbb{E} \left[(\hat{\mathbf{x}}_E - \mathbf{x}) (\mathbf{y}_E^G)^H \right] = \mathbf{0} \quad (30)$$

From (30), we find an expression of the equalizer as⁷:

$$\mathbf{G} = \sqrt{\alpha} \sigma_X^2 \Gamma_E^H \left(\alpha \sigma_X^2 \Gamma_E \Gamma_E^H + (1 - \alpha) |\mathbf{H}_E|^2 \sigma_{AN}^2 + \sigma_{V,E}^2 \mathbf{I}_Q \right)^{-1} \quad (31)$$

where $\sigma_X^2 \mathbf{I}_N = \mathbb{E} [\mathbf{x} \mathbf{x}^H]$. We remark from (31) that the implementation of the LMMSE requires at Eve the knowledge of \mathbf{H}_E as well as the AN energy σ_{AN}^2 .

So far, no analytic expression of the SINR has been found for the LMMSE implementation.

4.2 Optimal amount of AN to inject

This section is only dedicated for the scenarios where Eve implements the same decoding structure as Bob and a matched filtering decoder.

4.2.1 Eve's estimator: same structure as Bob

With (14), (17) and (22), it is possible to obtain a closed-form approximation of the SR upper bound and therefore to determine the amount of AN energy to inject that maximizes the SR. If we introduce $T_1 = -(U + 1)$, $T_2 = (U + 1)U\sigma_{V,E}^2 + (U + 1) - U\sigma_{V,B}^2$ and $T_3 = U\sigma_{V,B}^2(U\sigma_{V,E}^2 + 1)$, we obtain⁸:

$$C_s \lesssim \log_2 \left(\frac{\alpha^2 T_1 + \alpha T_2 + T_3}{T_3} \right) \quad (32)$$

Since T_3 is always strictly positive, the SR is maximized for:

$$\alpha_{\text{opt}} = \frac{-T_2}{2T_1} \quad (33)$$

4.2.2 Eve's estimator: matched filtering

With (14), (17) and (26), it is possible to obtain a closed-form approximation of the SR upper bound and therefore to determine the amount of AN energy to inject that maximizes the SR. If we introduce: $T_1 = U + 1$, $T_2 = (U + 1)^2 \sigma_E^2 + (U + 1) - U\sigma_B^2$, $T_3 = U(U + 1)\sigma_B^2 \sigma_E^2 + U\sigma_B^2$, and $T_4 = (U + 1)(U + 3)\sigma_B^2 - U\sigma_B^2$, we obtain⁹:

$$C_s \lesssim \log_2 \left(\frac{-\alpha^2 T_1 + \alpha T_2 + T_3}{\alpha T_4 + T_3} \right) \quad (34)$$

To maximize the secrecy rate as a function of the parameter α , we find the zeroes of:

$$\frac{\partial C_s}{\partial \alpha} = \frac{\frac{-\alpha^2 T_1 T_4 - 2\alpha T_1 T_3 + (T_2 T_3 - T_3 T_4)}{(\alpha T_4 + T_3)^2}}{\frac{-\alpha^2 T_1 + \alpha T_2 + T_3}{\alpha T_4 + T_3} \cdot \ln 2} \quad (35)$$

After some algebraic manipulations, one obtains:

$$\frac{\partial C_s}{\partial \alpha} = 0 \Leftrightarrow \alpha_{\text{opt}} = \frac{\pm \sqrt{T_1^2 T_3^2 + T_1 T_2 T_3 T_4 - T_1 T_3 T_4^2 - T_1 T_3}}{T_1 T_4} \quad (36)$$

where only the positive roots are solutions since $\alpha \in [0, 1]$.

⁷see Appendix A

⁸see Appendix B.1

⁹see Appendix B.2

4.3 Secrecy rate optimization via waterfilling

From section 4.2, the optimal amount of radiated energy dedicated for the transmission of the data signal is derived for the two models. The analytic expressions (33) and (36) lead to the coefficients α_{opt} that maximize the ergodic SR of the communication for two different decoding capabilities at Eve.

In the following, the optimization procedure will only be explained for the first decoding structure at Eve. The same discussion holds for the second one.

In this scenario, Eve only despread the received sequence. Before despreading, the signals at Bob and Eve are respectively given by:

$$\begin{aligned} \mathbf{y}_B &= \sqrt{\alpha_{\text{opt}}} |\mathbf{H}_B|^2 \mathbf{S} \mathbf{x} + \mathbf{v}_B \\ \mathbf{y}_E &= \sqrt{\alpha_{\text{opt}}} \mathbf{H}_E \mathbf{H}_B^* \mathbf{S} \mathbf{x} + \sqrt{1 - \alpha_{\text{opt}}} \mathbf{H}_E \mathbf{w} + \mathbf{v}_E \end{aligned} \quad (37)$$

We observe from (37) that an unique coefficient α_{opt} weights the Q components of the useful data. That is, each subcarrier will be affected by the same coefficient. However, we know that the channel capacity at one subcarrier is proportional to the subcarrier energy. Therefore, subcarriers with higher gains will contribute more to the total channel capacity than subcarriers with lower gains. We also consider throughout this paper that Alice can instantaneously estimate Bob's channel but does not have any information about Eve instantaneous CSI, such that we can compute the instantaneous capacity at Bob but we only have access to the ergodic capacity at Eve. From this discussion, we can state that, if we could have access to Eve's instantaneous capacity, we could tune the weights at each subcarrier, i.e., applying a different weight at each subcarrier depending on its power, in such a way that it enhances the instantaneous capacity at Bob and it degrades the instantaneous capacity at the eavesdropper position.

Since we only have access to the ergodic capacity at Eve, we proceed as follows:

Based on the statistics of Bob and Eve channels, we obtain a closed form expression of the ergodic SR given by (32). From that, we find via (33) the value of α_{opt} that, in the ergodic sense, will maximize the SR. Then, at each channel realization, we determine a new set of coefficients, denoted by $\boldsymbol{\alpha}_w = [\alpha_{w,0}, \dots, \alpha_{w,Q-1}]^T$, that enhances the instantaneous capacity at Bob while ensuring that:

1. The total radiated energy should remain constant:

$$\left| \sqrt{\alpha_{\text{opt}}} \mathbf{H}_B^* \mathbf{S} \mathbf{x} + \sqrt{1 - \alpha_{\text{opt}}} \odot \mathbf{w} \right|^2 = \left| \sqrt{\boldsymbol{\alpha}_w} \mathbf{H}_B^* \mathbf{S} \mathbf{x} + \sqrt{1 - \boldsymbol{\alpha}_w} \mathbf{w} \right|^2 \quad (38)$$

2. The energy radiated dedicated to the AN signal should remain constant:

$$\left| \sqrt{1 - \alpha_{\text{opt}}} \mathbf{w} \right|^2 = \left| \sqrt{1 - \boldsymbol{\alpha}_w} \odot \mathbf{w} \right|^2 \quad (39)$$

3. The AN signal should still lie in the null space of Bob:

$$\forall \epsilon > 0, \exists \boldsymbol{\alpha}_w : \mathbf{S}^H \mathbf{H}_B \sqrt{1 - \boldsymbol{\alpha}_w} \odot \mathbf{w} < \epsilon \quad (40)$$

Since we consider that Bob and Eve channels are independent, optimizing the coefficients that weight each subcarrier to enhance the capacity at Bob will not modify the capacity at Eve. In doing so, with the waterfilling optimization procedure, the SR will increase as it will be shown in section 5.2.3. However it is worth to note that this approach is computationally expensive since new weights have to be determined at each channel realization.

5 Simulation Results

A 256-subcarrier SISO OFDM system is considered. Bob and Eve channels are assumed to be uncorrelated. Each subcarrier is Rayleigh distributed and there is no correlation between subcarriers. As a reminder, the overall channel energies are normalized to unity for each channel realization. Bob's CSI is assumed to be perfectly known at Alice. Bob and Eve have the same level of noise. Simulations with 100 channel realizations and 300 OFDM blocks were performed using a 4-QAM modulation scheme.

5.1 Decoding results

The presented results in this section were obtained for the scenario where Eve has the same capabilities as Bob. This is subject to further completion where the different decoding structures will be included.

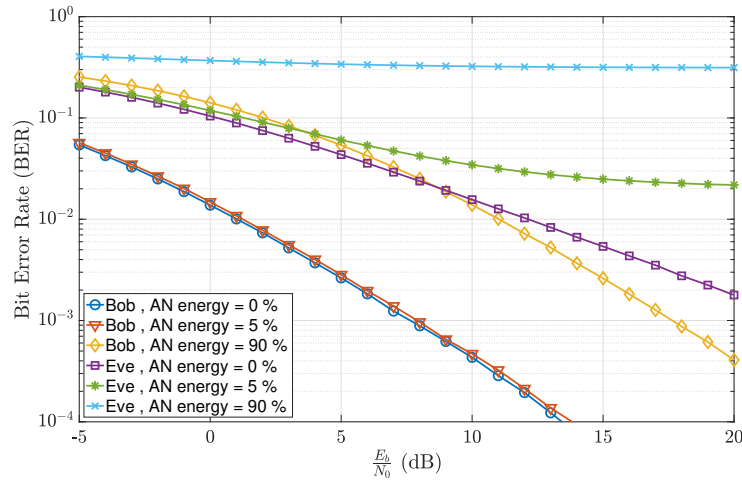


Figure 8: BER as a function of the level of noise for different AN energy values, BOR = 4

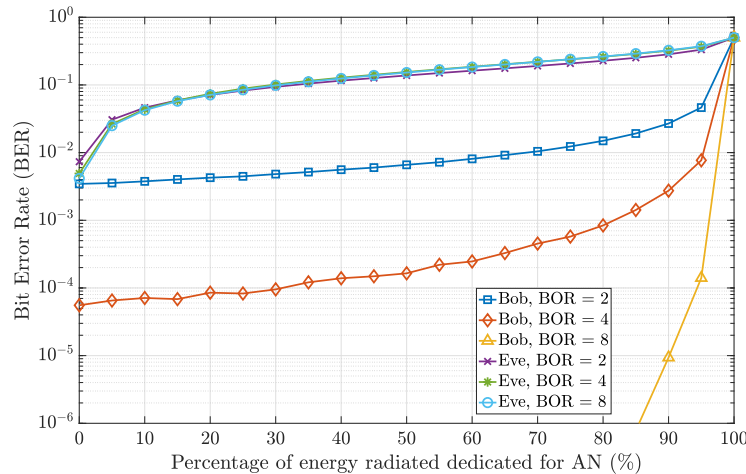


Figure 9: BER as a function of AN energy for different BOR values, $E_b/N_0 = 15\text{dB}$

Fig. 8 and 9 show the system performance in terms of BER obtained after ZF equalization at Bob and Eve. In Fig. 8, the BER is plotted as a function of E_b/N_0 , where E_b is the energy per bit, calculated after spreading, and N_0 is the noise power spectral density. Different levels of AN energy are investigated at fixed BOR. It can be observed that, as soon as a small amount of radiated energy is dedicated to AN, e.g., 5%, Eve's BER strongly increases. At the intended position, the BER also increases but much

slower. The reason is that the higher the percentage of energy dedicated to AN, the lower the received useful signal power at Bob. In Fig. 9, the BER is plotted as a function of the AN energy, at fixed $E_b/N_0 = 15$ dB and different BOR values. At the unintended position, the BER naturally increases with the amount of injected AN, whatever the BOR value. At Bob, low BER values can be maintained for high AN power by increasing the BOR. One can notice that, when $\alpha \rightarrow 0$, the BER curves all converge to 0.5, as expected.

5.2 Secrecy results

5.2.1 Comparison between models and simulations

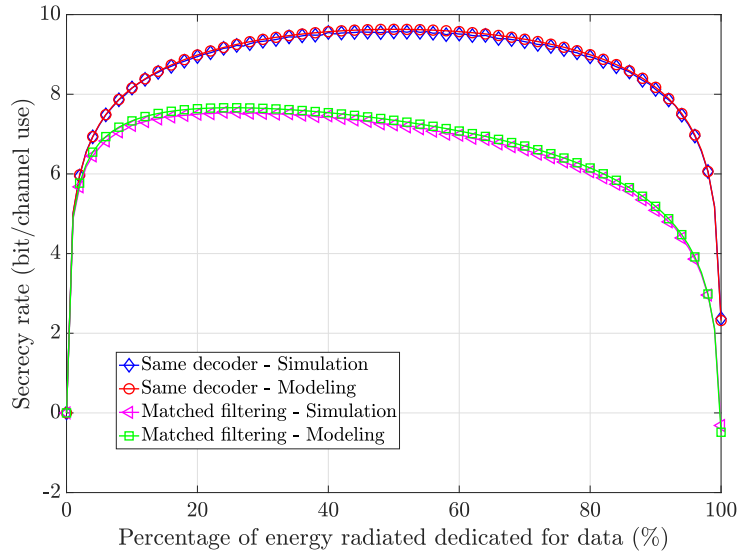


Figure 10: Secrecy Rate curves, analytic vs simulation for the 2 models, $E_b/N_0 = 25$ dB, BOR = 4

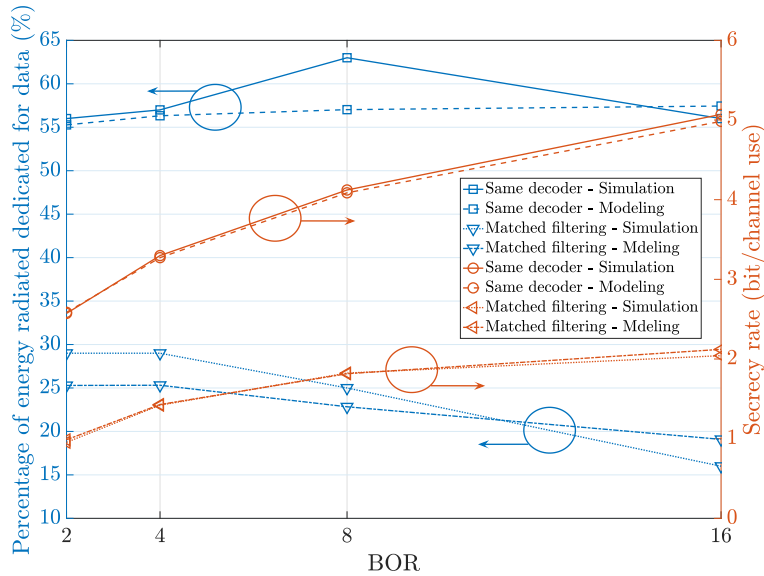


Figure 11: Optimal amount of AN to inject, Bob and Eve with the same decoding structure, $E_b/N_0 = 5$ dB

Fig. 10 shows the SR evolution as a function of α for the two derived models, i.e., Eve implementing a simple despreading, and Eve implementing a matched filter. First, it can be seen that analytic curves, given by (32) and (34), approximate well the simulation curves and remain tight upper bounds for

both models. In addition, the SR obtained with the classical FD TR SISO OFDM system, i.e., no AN signal, is enhanced with the addition of AN except for very high percentages of AN. Furthermore, for both models, no more secrecy is obtained when $\alpha \rightarrow 0$, since the SINR's at Bob and Eve drop to zero. When Eve implements a matched filtering decoder, we observe that, when $\alpha \rightarrow 1$, i.e., no AN energy is injected, the SR becomes negative. It first shows that implementing a matched filter at the receiver side is more advantageous than implementing it at the transmitter, but above all, that the injection of AN is essential when Eve implements a matched filter to ensure a positive SR.

The left y -axis of Fig.11 illustrates the values of α_{opt} given by (33) and (36) that maximize the SR determined from the closed-form approximations (32) and (34), as well as obtained from the numerical simulations. The analytic estimations of the optimal amount of AN energy are not perfect but, the resulting simulated SR are very close to the maximal SR obtained numerically, as it can be observed on the right y -axis of Fig.11. The reason can be observed in Fig. 10 where the SR vary very slowly about their maxima when α changes, for both models. So, for a given BOR value, Alice can make a rough determination of α_{opt} depending on Eve decoding structure, and therefore the available SR, if E_b/N_0 is known. One can also note that much lower values of α_{opt} , i.e. higher AN energy, should be injected to maximize the SR when Eve matched filters the received signal compared to the scenario where Eve implements the same decoder as Bob.

5.2.2 Comparison between the different decoding structures

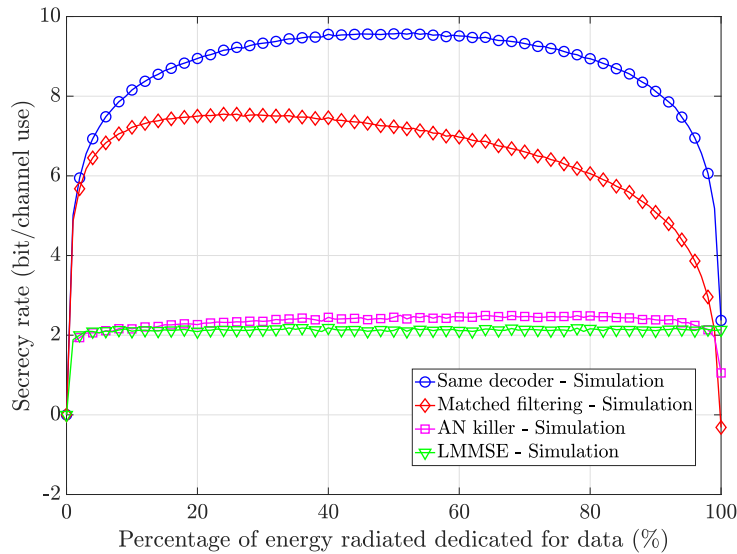


Figure 12: Secrecy Rate curves for the different decoding structures at Eve, $E_b/N_0 = 25$ dB, BOR = 4

Fig.12 shows the secrecy performances for the 4 different structures implemented at the eavesdropper position, each of them assuming more computational resources and/or more knowledges at Eve as compared to Bob. It can be seen that when Eve implements the same receiving structure as Bob, the SR is very high compared to the other curves, as anticipated from Section 4.1.2.1. When the AN killer algorithm is implemented, we observe that the curve remains flat, except for the situation where all the radiated energy is dedicated for the AN signal. The reason is that Eve's noise is amplify whatever the value of α since the AN signal is suppressed. The LMMSE curves exhibit the lower SR since it performs a decoding tradeoff between suppressing the AN and amplifying the noise, except for very high

percentages of energy dedicated to the useful signal. Finally, we note that the SR when Eve implements a matched filter is relatively low. Furthermore, it becomes negative when the transmitted signal only contains data. In fact, if we assume that the additive noise at Bob and Eve have the same relative energy, the SINR ratio when no AN is radiated becomes:

$$\frac{\mathbb{E}[\gamma_{B,n}]}{\mathbb{E}[\gamma_{E,n}]} \Big|_{\alpha \rightarrow 1} \approx \frac{\frac{U+1}{U}}{\frac{U+3}{U}} = \frac{U+1}{U+3} < 1 \quad (41)$$

leading to a negative SR. From that we conclude that performing a matched filter at the receiving side gives to Eve an advantage compared to Bob.

5.2.3 Waterfilling Optimization

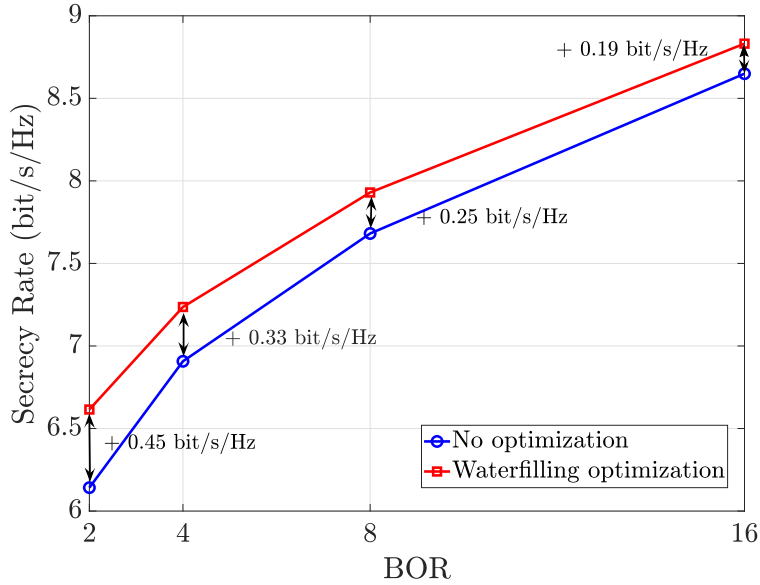


Figure 13: SR optimization via waterfilling, Bob and Eve with same capabilities, $E_b/N_0 = 20$ dB

Fig. 13 presents the maximal values of the SR obtained when Eve implements the despreading only receiving structure, i.e. the same structure as Bob, before and after waterfilling optimization. As a reminder, before and after optimization, the mean energy radiated dedicated to the useful data remains unchanged. This amount of energy is computed thanks to (33) in order to ensure a maximal SR. This SR is then further increased via the waterfilling optimization procedure, as described in section 4.3. As we can see, there is an increase of the SR for all BOR values thanks to the optimization. However, this increase decreases with an increase of the BOR. This can be explained since, when the BOR increases, the channel frequency diversity is better exploited by the TR scheme. Therefore, it becomes more difficult to gain from the coefficient optimization procedure and the SR is then less enhanced.

6 Conclusion & Perspectives

The problem of securing the FD TR SISO OFDM wireless transmission from a transmitter to a legitimate receiver in the presence of a passive eavesdropper is considered. A novel and original approach based on the addition of an AN signal onto OFDM blocks that improves the PLS is proposed. This approach can be easily integrated into existing standards based on OFDM. It only requires a single transmit antenna and is therefore well suited for devices with limited capabilities. Analytic and simulation results show

that the novel approach significantly improves the security of the communication and so considerably jeopardizes any attempt of an eavesdropper to retrieve the data.

In this work, four eavesdropper decoding structures are investigated giving rise to different secrecy performances. From the previous discussion, we remark that a simple matched filtering decoding structure strongly impacts the secrecy rate of the communication. As a result, one of the aspects of the future work will be to implement a more robust scheme. New AN injection methods and/or new precoding techniques will be investigated to try to further improve the security of the communication.

So far, only a SISO system has been considered. A natural extension of the work will be to consider a MIMO system. That way, in addition to benefiting from the frequency diversity of the channels, we will benefit from the spatial diversity. In doing so, any attempt to try to eavesdrop the data will be expected to become harder. In addition, we will consider that the passive eavesdropper will be equipped with multiple antennas which will gives him more decoding capabilities.

Furthermore, only a single-user communication is now considered. A multi-users scheme can be designed where each user channel can contribute to secure the whole communication. As a consequence, the level of security of the scheme is expected to improve.

At this point of the work, a very simple channel model was implemented. In fact, a multi-taps channel where each tap is Rayleigh distributed is considered. No correlation between the different subcarriers, i.e. frequency correlation, or spatial correlation between Bob and Eve channels have been taken into account. This leads to results that are relatively easy to compare with analytic models but that do not represent well real life scenarios. A natural extension of the work will be to consider these correlations in order to obtain more realistic results.

Finally, the objective will be to test the FD TR OFDM system with the Universal Software Radio Peripheral (USRP) devices in real indoor environments.

References

- [1] H. Alves, R. D. Souza, M. Debbah, and M. Bennis, "Performance of transmit antenna selection physical layer security schemes," *IEEE Signal Processing Letters*, vol. 19, no. 6, pp. 372–375, 2012.
- [2] N. Yang, H. A. Suraweera, I. B. Collings, and C. Yuen, "Physical layer security of tas/mrc with antenna correlation," *IEEE Transactions on Information Forensics and Security*, vol. 8, no. 1, pp. 254–259, 2012.
- [3] D.-D. Tran, D.-B. Ha, V. Tran-Ha, and E.-K. Hong, "Secrecy analysis with mrc/sc-based eavesdropper over heterogeneous channels," *IETE Journal of Research*, vol. 61, no. 4, pp. 363–371, 2015.
- [4] A. D. Wyner, "The wire-tap channel," *Bell system technical journal*, vol. 54, no. 8, pp. 1355–1387, 1975.
- [5] M. Li, S. Kundu, D. A. Pados, and S. N. Batalama, "Waveform design for secure siso transmissions and multicasting," *IEEE Journal on Selected Areas in Communications*, vol. 31, no. 9, pp. 1864–1874, 2013.
- [6] Q. Xu, P. Ren, Q. Du, and L. Sun, "Security-aware waveform and artificial noise design for time-reversal-based transmission," *IEEE Transactions on Vehicular Technology*, vol. 67, no. 6, pp. 5486–5490, 2018.
- [7] S. Li, N. Li, X. Tao, Z. Liu, H. Wang, and J. Xu, "Artificial noise inserted secure communication in time-reversal systems," in *2018 IEEE Wireless Communications and Networking Conference (WCNC)*. IEEE, 2018, pp. 1–6.
- [8] S. Li, N. Li, Z. Liu, H. Wang, J. Xu, and X. Tao, "Artificial noise aided path selection for secure tr communications," in *2017 IEEE/CIC International Conference on Communications in China (ICCC)*. IEEE, 2017, pp. 1–6.
- [9] C. Oestges, A. D. Kim, G. Papanicolaou, and A. J. Paulraj, "Characterization of space-time focusing in time-reversed random fields," *IEEE transactions on antennas and propagation*, vol. 53, no. 1, pp. 283–293, 2005.
- [10] T.-H. Nguyen, J.-F. Determe, M. Van Eeckhaute, J. Louveaux, P. De Doncker, and F. Horlin, "Frequency-domain time-reversal precoding in wideband miso ofdm communication systems," *arXiv preprint arXiv:1904.10727*, 2019.
- [11] T. Dubois, M. Crussiere, and M. Helard, "On the use of time reversal for digital communications with non-impulsive waveforms," in *2010 4th International Conference on Signal Processing and Communication Systems*. IEEE, 2010, pp. 1–6.
- [12] S. Ahmed, T. Noguchi, and M. Kawai, "Selection of spreading codes for reduced papr in mc-cdma systems," in *2007 IEEE 18th International Symposium on Personal, Indoor and Mobile Radio Communications*, 2007, pp. 1–5.
- [13] H. Tran, H. Tran, G. Kaddoum, D. Tran, and D. Ha, "Effective secrecy-sinr analysis of time reversal-employed systems over correlated multi-path channel," in *2015 IEEE 11th International Conference on Wireless and Mobile Computing, Networking and Communications (WiMob)*, 2015, pp. 527–532.

Appendices

A SINR derivation

Let A and B be 2 RV's. These basics properties will be used:

$$\begin{aligned}\mathbb{E} [\alpha A + \beta B] &= \alpha \mathbb{E} [A] + \beta \mathbb{E} [B] \quad \alpha, \beta \in \mathbb{R} \\ \mathbb{E} [AB] &= \mathbb{E} [A] \mathbb{E} [B] \quad \text{if } A \text{ and } B \text{ are independent} \\ \mathbb{E} [AB] &= \mathbb{E} [A] \mathbb{E} [B] + \text{cov}(A, B) \quad \text{if } A \text{ and } B \text{ are correlated}\end{aligned}\tag{A.1}$$

A.1 At the intended position

As a recall, the received sequence is given by:

$$\mathbf{y}_B^H = \sqrt{\alpha} \mathbf{S}^H |\mathbf{H}_B|^2 \mathbf{S} \mathbf{x} + \mathbf{S}^H \mathbf{v}_B\tag{A.2}$$

Data component

From (15) and (16), we have:

$$\mathbb{E} [k^2] = \mathbb{E} \left[\left| \sqrt{\alpha} \mathbf{S}^H |\mathbf{H}_B|^2 \mathbf{S} \right|^2 \right]\tag{A.3a}$$

$$\mathbb{E} [k_n^2] = \mathbb{E} \left[\left| \frac{\sqrt{\alpha}}{U} \sum_{i=0}^{U-1} |h_{B,n+iN}|^2 \right|^2 \right]\tag{A.3b}$$

$$= \frac{\alpha}{U^2} \mathbb{E} \left[\left(\sum_{i=0}^{U-1} |h_{B,n+iN}|^2 \right) \left(\sum_{j=0}^{U-1} |h_{B,n+jN}|^2 \right)^H \right]\tag{A.3c}$$

$$= \frac{\alpha}{U^2} \mathbb{E} \left[\sum_{i=0}^{U-1} \sum_{j=0}^{U-1} |h_{B,n+iN}|^2 |h_{B,n+jN}^*|^2 \right]\tag{A.3d}$$

$$= \frac{\alpha}{U^2} \mathbb{E} \left[\sum_{i=0}^{U-1} |h_{B,n+iN}|^4 + \sum_{i=0}^{U-1} \sum_{\substack{j=0 \\ j \neq i}}^{U-1} |h_{B,n+iN}|^2 |h_{B,n+jN}^*|^2 \right]\tag{A.3e}$$

$$= \frac{\alpha}{U^2} \left(\mathbb{E} \left[\sum_{i=0}^{U-1} |h_{B,n+iN}|^4 \right] + \mathbb{E} \left[\sum_{i=0}^{U-1} \sum_{\substack{j=0 \\ j \neq i}}^{U-1} |h_{B,n+iN}|^2 |h_{B,n+jN}^*|^2 \right] \right)\tag{A.3f}$$

$$= \frac{\alpha}{U^2} \left(\mathbb{E} \left[\sum_{i=0}^{U-1} |h_{B,n+iN}|^4 \right] + \mathbb{E} \left[\sum_{i=0}^{U-1} |h_{B,n+iN}|^2 \right] \mathbb{E} \left[\sum_{\substack{j=0 \\ j \neq i}}^{U-1} |h_{B,n+jN}^*|^2 \right] \right)\tag{A.3g}$$

$$= \frac{\alpha}{U^2} (2U + U(U-1)) = \frac{\alpha(U+1)}{U}\tag{A.3h}$$

Going from (A.3g) to (A.3h) can be deduced from Appendix C. It is then easy to show that $\mathbb{E} [|h_{B,n+iN}|^4] = 2$.

Additive white gaussian noise component

We compute the mean energy per symbol of the received noise signal:

$$\mathbb{E} \left[|\mathbf{v}_B|^2 \right] = \mathbb{E} \left[\left| \mathbf{S}^H \mathbf{v}_B \right|^2 \right] \quad (\text{A.4a})$$

$$= \mathbb{E} \left[\left(\mathbf{S}^H \mathbf{v}_B \right) \left(\mathbf{S}^H \mathbf{v}_B \right)^H \right] \quad (\text{A.4b})$$

$$= \mathbb{E} \left[\mathbf{S}^H \mathbf{v}_B \mathbf{v}_B^* \mathbf{S} \right] \quad (\text{A.4c})$$

$$\mathbb{E} \left[|v_{B,n}|^2 \right] = \frac{1}{U} \mathbb{E} \left[\sum_{i=0}^{U-1} |v_{B,n+iN}|^2 \right] = \sigma_{V,B}^2 \quad (\text{A.4d})$$

A.2 At the unintended position

At the unintended position, the received signal is given by:

$$\mathbf{y}_E^G = \sqrt{\alpha} \mathbf{G} \Gamma_E \mathbf{x} + \sqrt{1-\alpha} \mathbf{G} \mathbf{H}_E \mathbf{w} + \mathbf{v}_E \quad (\text{A.5})$$

where $\Gamma_E = \mathbf{H}_E \mathbf{H}_E^* \mathbf{S}$

A.2.1 Eve and Bob with identical capacities

In this scenario, we have:

$$\mathbf{y}_E^G = \sqrt{\alpha} \mathbf{S}^H \Gamma_E \mathbf{S} \mathbf{x} + \sqrt{1-\alpha} \mathbf{S}^H \mathbf{H}_E \mathbf{w} + \mathbf{S}^H \mathbf{v}_E \quad (\text{A.6})$$

Data component

From (21), we have:

$$\mathbb{E} \left[|\mathbf{A}_1|^2 \right] = \mathbb{E} \left[\left| \sqrt{\alpha} \mathbf{S}^H \mathbf{H}_E \mathbf{H}_B^* \mathbf{S} \right|^2 \right] \quad (\text{A.7a})$$

$$= \alpha \mathbb{E} \left[\left(\mathbf{S}^H \mathbf{H}_E \mathbf{H}_B^* \mathbf{S} \right) \left(\mathbf{S}^H \mathbf{H}_E \mathbf{H}_B^* \mathbf{S} \right)^H \right] \quad (\text{A.7b})$$

$$\mathbb{E} \left[|A_{1,n}|^2 \right] = \alpha \mathbb{E} \left[\frac{1}{U^2} \sum_{i=0}^{U-1} |h_{E,n+iN}|^2 |h_{B,n+iN}^*|^2 \right] \quad (\text{A.7c})$$

$$= \frac{\alpha}{U} \quad (\text{A.7d})$$

Additive white gaussian noise component

For the noise component:

$$\mathbb{E} \left[|\mathbf{A}_2|^2 \right] = \mathbb{E} \left[\left| \mathbf{S}^H \mathbf{v}_E \right|^2 \right] \quad (\text{A.8a})$$

$$= \mathbb{E} \left[\left(\mathbf{S}^H \mathbf{v}_E \right) \left(\mathbf{S}^H \mathbf{v}_E \right)^H \right] \quad (\text{A.8b})$$

$$= \mathbb{E} \left[\mathbf{S}^H \mathbf{v}_E \mathbf{v}_E^* \mathbf{S} \right] \quad (\text{A.8c})$$

$$\mathbb{E} \left[|A_{2,n}|^2 \right] = \frac{1}{U} \mathbb{E} \left[\sum_{i=0}^{U-1} |v_{E,n+iN}|^2 \right] = \sigma_{V,E}^2 \quad (\text{A.8d})$$

Artificial noise component

The AN term is given by:

$$\mathbb{E} [|\mathbf{A}_3|^2] = \mathbb{E} \left[\left| \sqrt{1-\alpha} \mathbf{S}^H \mathbf{H}_E \mathbf{w} \right|^2 \right] \quad (\text{A.9a})$$

$$= (1-\alpha) \mathbb{E} \left[\left(\mathbf{S}^H \mathbf{H}_E \mathbf{w} \right) \left(\mathbf{S}^H \mathbf{H}_E \mathbf{w} \right)^H \right] \quad (\text{A.9b})$$

$$= (1-\alpha) \mathbb{E} \left[\mathbf{S}^H \mathbf{H}_E \mathbf{H}_E^* \mathbf{w} \mathbf{w}^* \mathbf{S} \right] \quad (\text{A.9c})$$

$$\mathbb{E} [|A_{3,n}|^2] = \frac{1-\alpha}{U} \mathbb{E} \left[\sum_{i=0}^{U-1} |h_{E,n+iN} w_{n+iN}|^2 \right] = (1-\alpha) \sigma_{\text{AN}}^2 \quad (\text{A.9d})$$

A.2.2 Matched Filtering

When Eve performs a matched filtering with the received signal, we obtain:

$$\mathbf{y}_E^G = \sqrt{\alpha} \mathbf{S}^H |\mathbf{H}_E|^2 |\mathbf{H}_B|^2 \mathbf{S} \mathbf{x} + \sqrt{1-\alpha} \mathbf{S}^H \mathbf{H}_B |\mathbf{H}_E|^2 \mathbf{w} + \mathbf{S}^H \mathbf{H}_E^* \mathbf{H}_B \mathbf{v}_E \quad (\text{A.10})$$

Data component

The data component is given by:

$$\mathbb{E} [|\mathbf{A}_1|^2] = \mathbb{E} \left[\left| \sqrt{\alpha} \mathbf{S}^H |\mathbf{H}_E|^2 |\mathbf{H}_B|^2 \mathbf{S} \mathbf{x} \right|^2 \right] \quad (\text{A.11a})$$

$$= \alpha \mathbb{E} \left[\left| \mathbf{S}^H |\mathbf{H}_E|^2 |\mathbf{H}_B|^2 \mathbf{S} \right|^2 \right] \mathbb{E} [|\mathbf{x}|^2] \quad (\text{A.11b})$$

$$\mathbb{E} [|A_{1,n}|^2] = \alpha \mathbb{E} \left[\left| \frac{1}{U} \sum_{i=0}^{U-1} |h_{B,n+iN}|^2 |h_{E,n+iN}|^2 \right|^2 \right] \quad (\text{A.11c})$$

$$= \frac{\alpha}{U^2} \mathbb{E} \left[\left(\sum_{i=0}^{U-1} |h_{B,n+iN}|^2 |h_{E,n+iN}|^2 \right) \left(\sum_{j=0}^{U-1} |h_{B,n+jN}|^2 |h_{E,n+jN}|^2 \right)^H \right] \quad (\text{A.11d})$$

$$= \frac{\alpha}{U^2} \mathbb{E} \left[\sum_{i=0}^{U-1} \sum_{j=0}^{U-1} |h_{B,n+jN}|^2 |h_{E,n+iN}|^2 |h_{B,n+jN}^*|^2 |h_{E,n+iN}^*|^2 \right] \quad (\text{A.11e})$$

$$= \frac{\alpha}{U^2} \left(\sum_{i=0}^{U-1} |h_{B,n+iN}|^4 |h_{E,n+iN}|^4 + \sum_{i=0}^{U-1} \sum_{\substack{j=0 \\ j \neq i}}^{U-1} |h_{B,n+jN}|^2 |h_{E,n+iN}|^2 |h_{B,n+jN}^*|^2 |h_{E,n+iN}^*|^2 \right) \quad (\text{A.11f})$$

$$= \frac{\alpha}{U^2} (U \cdot 2 + U(U-1)) = \frac{\alpha(U+3)}{U} \quad (\text{A.11g})$$

We remark that (A.11d) can be directly computed from (A.3c), which leads to (A.11g).

Additive white gaussian noise component

The noise component is:

$$\mathbb{E} \left[|\mathbf{A}_2|^2 \right] = \mathbb{E} \left[\left| \mathbf{S}^H \mathbf{H}_E^* \mathbf{H}_B \mathbf{v}_E \right|^2 \right] \quad (\text{A.12a})$$

$$= \mathbb{E} \left[\left(\mathbf{S}^H \mathbf{H}_E^* \mathbf{H}_B \mathbf{v}_E \right) \left(\mathbf{S}^H \mathbf{H}_E^* \mathbf{H}_B \mathbf{v}_E \right)^H \right] \quad (\text{A.12b})$$

$$= \mathbb{E} \left[\mathbf{S}^H \mathbf{H}_E \mathbf{H}_E^* \mathbf{H}_B \mathbf{H}_B^* \mathbf{v}_E \mathbf{v}_E^* \mathbf{S} \right] \quad (\text{A.12c})$$

$$\mathbb{E} \left[|A_{2,n}|^2 \right] = \frac{1}{U} \mathbb{E} \left[\sum_{i=0}^{U-1} |h_{E,n+iN}|^2 |h_{B,n+iN}|^2 |v_{E,n+iN}|^2 \right] = \sigma_{V,E}^2 \quad (\text{A.12d})$$

Artificial noise component

We want to compute the mean energy per symbol received at Eve for the AN component when she performs a matched filtering. The AN term at Eve is given by:

$$\mathbf{v} = \mathbf{S}^H \mathbf{H}_B |\mathbf{H}_E|^2 \mathbf{w} \quad (\text{A.13a})$$

$$= \mathbf{A} |\mathbf{H}_E|^2 \mathbf{V}_2 \mathbf{w}' \quad (\text{A.13b})$$

$$= \mathbf{U} \begin{pmatrix} \mathbf{\Sigma} & \mathbf{0}_{Q-N \times N} \end{pmatrix} \begin{pmatrix} \mathbf{V}_1^H \\ \mathbf{V}_2^H \end{pmatrix} |\mathbf{H}_E|^2 \mathbf{V}_2 \mathbf{w}' \quad (\text{A.13c})$$

$$= \mathbf{U} \mathbf{\Sigma} \mathbf{V}_1^H |\mathbf{H}_E|^2 \mathbf{V}_2 \mathbf{w}' \quad (\text{A.13d})$$

where:

- \mathbf{U} is a $N \times N$ unitary matrix, i.e., $\mathbf{U}^H \mathbf{U} = \mathbf{I}_N$, its columns form an orthonormal basis of \mathcal{C}^N and are the left singular vectors of each singular value of \mathbf{A} ;
- $\mathbf{\Sigma}$ is a $N \times N$ diagonal matrix containing the singular values of \mathbf{A} in the descending order, i.e., $\sigma_i = \Sigma_{i,i}$;
- \mathbf{V}_1 is a $Q \times N$ complex matrix that contains the right singular vectors associated to the non-zero singular values;
- \mathbf{V}_2 is a $Q \times Q - N$ complex matrix that contains the right singular vectors associated to the zeroes singular values, i.e., that span the right null-space of \mathbf{A} ;
- $\mathbf{V} = (\mathbf{V}_1 \mathbf{V}_2)$ is a $Q \times Q$ unitary matrix, i.e., $\mathbf{V}^H \mathbf{V} = \mathbf{I}_Q$, its columns form an orthonormal basis of \mathcal{C}^Q and are the right singular vectors of each singular value of \mathbf{A} ;
- \mathbf{w}' is a $Q - N \times 1$ complex normal random variable such that $\mathbf{w}' \sim \mathcal{CN}(0, 1)$

Note that going from (A.13a) to (A.13b), we deliberately omit the weighting coefficient β appearing in (9) for the sake of simplicity. The value of this coefficient will be given at the end of the discussion.

Let us now look at the covariance matrix

$$\mathbb{E} (\mathbf{v} \mathbf{v}^H) = \mathbb{E} \left(\mathbf{U} \mathbf{\Sigma} \mathbf{V}_1^H |\mathbf{H}_E|^2 \mathbf{V}_2 \mathbf{w}' \left(\mathbf{U} \mathbf{\Sigma} \mathbf{V}_1^H |\mathbf{H}_E|^2 \mathbf{V}_2 \mathbf{w}' \right)^H \right) \quad (\text{A.14a})$$

$$= \mathbb{E} \left(\mathbf{U} \mathbf{\Sigma} \mathbf{V}_1^H |\mathbf{H}_E|^2 \mathbf{V}_2 \mathbf{w}' \mathbf{w}'^H \mathbf{V}_2^H |\mathbf{H}_E|^2 \mathbf{V}_1 \mathbf{\Sigma}^H \mathbf{U}^H \right) \quad (\text{A.14b})$$

Note that \mathbf{w}' is independent of other random variables and has a unit covariance matrix. We can thus put the expectation inside to get

$$\mathbb{E}(\mathbf{v}\mathbf{v}^H) = \mathbb{E}\left(\mathbf{U}\Sigma\mathbf{V}_1^H|\mathbf{H}_E|^2\mathbf{V}_2\mathbf{V}_2^H|\mathbf{H}_E|^2\mathbf{V}_1\Sigma^H\mathbf{U}^H\right) \quad (\text{A.15})$$

We rewrite $|\mathbf{H}_E|^2 = \sum_{q=1}^Q |H_{E,q}|^2 \mathbf{e}_q \mathbf{e}_q^T$ where \mathbf{e}_q is an all zero vector except a 1 at row q to isolate the independent random variable H_E

$$\mathbb{E}(\mathbf{v}\mathbf{v}^H) = \sum_{q=1}^Q \sum_{q'=1}^Q \mathbb{E}(|H_{E,q}|^2 |H_{E,q'}|^2) \mathbb{E}\left(\mathbf{U}\Sigma\mathbf{V}_1^H \mathbf{e}_q \mathbf{e}_q^T \mathbf{V}_2 \mathbf{V}_2^H \mathbf{e}_{q'} \mathbf{e}_{q'}^T \mathbf{V}_1 \Sigma^H \mathbf{U}^H\right) \quad (\text{A.16a})$$

$$= \sum_{q=1}^Q \mathbb{E}(|H_{E,q}|^4) \mathbb{E}\left(\mathbf{U}\Sigma\mathbf{V}_1^H \mathbf{e}_q \mathbf{e}_q^T \mathbf{V}_2 \mathbf{V}_2^H \mathbf{e}_q \mathbf{e}_q^T \mathbf{V}_1 \Sigma^H \mathbf{U}^H\right) \quad (\text{A.16b})$$

$$+ \sum_{q=1}^Q \sum_{q' \neq q}^Q \mathbb{E}(|H_{E,q}|^2 |H_{E,q'}|^2) \mathbb{E}\left(\mathbf{U}\Sigma\mathbf{V}_1^H \mathbf{e}_q \mathbf{e}_q^T \mathbf{V}_2 \mathbf{V}_2^H \mathbf{e}_{q'} \mathbf{e}_{q'}^T \mathbf{V}_1 \Sigma^H \mathbf{U}^H\right) \quad (\text{A.16c})$$

$$= 2 \sum_{q=1}^Q \mathbb{E}\left(\mathbf{U}\Sigma\mathbf{V}_1^H \mathbf{e}_q \mathbf{e}_q^T \mathbf{V}_2 \mathbf{V}_2^H \mathbf{e}_q \mathbf{e}_q^T \mathbf{V}_1 \Sigma^H \mathbf{U}^H\right) \quad (\text{A.16d})$$

$$+ \sum_{q=1}^Q \sum_{q' \neq q}^Q \mathbb{E}\left(\mathbf{U}\Sigma\mathbf{V}_1^H \mathbf{e}_q \mathbf{e}_q^T \mathbf{V}_2 \mathbf{V}_2^H \mathbf{e}_{q'} \mathbf{e}_{q'}^T \mathbf{V}_1 \Sigma^H \mathbf{U}^H\right) \quad (\text{A.16e})$$

$$= \sum_{q=1}^Q \mathbb{E}\left(\mathbf{U}\Sigma\mathbf{V}_1^H \mathbf{e}_q \mathbf{e}_q^T \mathbf{V}_2 \mathbf{V}_2^H \mathbf{e}_q \mathbf{e}_q^T \mathbf{V}_1 \Sigma^H \mathbf{U}^H\right) \quad (\text{A.16f})$$

$$+ \mathbb{E}\left(\mathbf{U}\Sigma\mathbf{V}_1^H \sum_{q=1}^Q \mathbf{e}_q \mathbf{e}_q^T \mathbf{V}_2 \mathbf{V}_2^H \sum_{q'=1}^Q \mathbf{e}_{q'} \mathbf{e}_{q'}^T \mathbf{V}_1 \Sigma^H \mathbf{U}^H\right) \quad (\text{A.16g})$$

$$= \sum_{q=1}^Q \mathbb{E}\left(\mathbf{U}\Sigma\mathbf{V}_1^H \mathbf{e}_q \mathbf{e}_q^T \mathbf{V}_2 \mathbf{V}_2^H \mathbf{e}_q \mathbf{e}_q^T \mathbf{V}_1 \Sigma^H \mathbf{U}^H\right) + \mathbb{E}\left(\mathbf{U}\Sigma\mathbf{V}_1^H \mathbf{V}_2 \mathbf{V}_2^H \mathbf{V}_1 \Sigma^H \mathbf{U}^H\right) \quad (\text{A.16h})$$

Using the fact that $\mathbf{V}_2^H \mathbf{V}_1 = \mathbf{0}$, the second term cancels and

$$\mathbb{E}(\mathbf{v}\mathbf{v}^H) = \mathbb{E}\left(\mathbf{U}\Sigma\mathbf{V}_1^H \sum_{q=1}^Q \left(\mathbf{e}_q \mathbf{e}_q^T \mathbf{V}_2 \mathbf{V}_2^H \mathbf{e}_q \mathbf{e}_q^T\right) \mathbf{V}_1 \Sigma^H \mathbf{U}^H\right) \quad (\text{A.17})$$

Since all elements of \mathbf{v} have same variance, we can compute it as

$$\frac{1}{N} \mathbb{E}(\|\mathbf{v}\|^2) = \frac{1}{N} \mathbb{E}(\mathbf{v}\mathbf{v}^H) \quad (\text{A.18a})$$

$$= \frac{1}{N} \mathbb{E}\left(\Sigma^2 \mathbf{V}_1^H \sum_{q=1}^Q \left(\mathbf{e}_q \mathbf{e}_q^T \mathbf{V}_2 \mathbf{V}_2^H \mathbf{e}_q \mathbf{e}_q^T\right) \mathbf{V}_1\right) \quad (\text{A.18b})$$

Let us rewrite $\mathbf{V}_1 = \sum_l \mathbf{e}_l \mathbf{v}_{1,l}^H$ where $\mathbf{v}_{1,l}^H$ is the l -th row of \mathbf{V}_1 (of dimension $N \times 1$) with only one nonzero element.

$$\frac{1}{N} \mathbb{E}(\|\mathbf{v}\|^2) = \frac{1}{N} \sum_{q=1}^Q \sum_l \sum_{l'} \mathbb{E}\left(\Sigma^2 \mathbf{v}_{1,l} \mathbf{e}_{l'}^T \mathbf{e}_q \mathbf{e}_q^T \mathbf{V}_2 \mathbf{V}_2^H \mathbf{e}_q \mathbf{e}_q^T \mathbf{e}_l \mathbf{v}_{1,l}^H\right) \quad (\text{A.19a})$$

$$= \frac{1}{N} \sum_{q=1}^Q \sum_l \sum_{l'} \delta_{l'-q} \delta_{l-q} \mathbb{E}\left(\Sigma^2 \mathbf{v}_{1,l} \mathbf{e}_q^T \mathbf{V}_2 \mathbf{V}_2^H \mathbf{e}_q \mathbf{v}_{1,l}^H\right) \quad (\text{A.19b})$$

$$= \frac{1}{N} \sum_{q=1}^Q \mathbb{E}\left(\Sigma^2 \mathbf{v}_{1,q} \mathbf{e}_q^T \mathbf{V}_2 \mathbf{V}_2^H \mathbf{e}_q \mathbf{v}_{1,q}^H\right) \quad (\text{A.19c})$$

Let us rewrite $\mathbf{V}_2 = \sum_l \mathbf{e}_l \mathbf{v}_{2,l}^H$ where $\mathbf{v}_{2,l}^H$ is the l -th row of \mathbf{V}_2 (of dimension $Q - N \times 1$) with $U - 1$ nonzero elements

$$\frac{1}{N} \mathbb{E} (\|\mathbf{v}\|^2) = \frac{1}{N} \sum_{q=1}^Q \sum_l \sum_{l'} \mathbb{E} \left(\Sigma^2 \mathbf{v}_{1,q} \mathbf{e}_q^T \mathbf{e}_l \mathbf{v}_{2,l}^H \mathbf{v}_{2,l'} \mathbf{e}_{l'}^T \mathbf{e}_q \mathbf{v}_{1,q}^H \right) \quad (\text{A.20a})$$

$$= \frac{1}{N} \sum_{q=1}^Q \mathbb{E} \left(\Sigma^2 \mathbf{v}_{1,q} \mathbf{v}_{2,q}^H \mathbf{v}_{2,q} \mathbf{v}_{1,q}^H \right) \quad (\text{A.20b})$$

$$= \frac{1}{N} \sum_{q=1}^Q \mathbb{E} \left(\|\mathbf{v}_{2,q}\|^2 \mathbf{v}_{1,q}^H \Sigma^2 \mathbf{v}_{1,q} \right) \quad (\text{A.20c})$$

where $\mathbf{v}_{1,q}^H \Sigma^2 \mathbf{v}_{1,q} \|\mathbf{v}_{1,q}\|^2 \sigma_n^2$ is a scalar. Therefore, we obtain:

$$\frac{1}{N} \mathbb{E} (\|\mathbf{v}\|^2) = \frac{1}{N} \sum_{q=1}^Q \mathbb{E} \left(\|\mathbf{v}_{2,q}\|^2 \|\mathbf{v}_{1,q}\|^2 \sigma_n^2 \right) \quad (\text{A.21})$$

Since \mathbf{V} forms an orthonormal basis, i.e., $\mathbf{V}^H \mathbf{V} = \mathbf{I}_Q$, we have $\|\mathbf{v}_{1,q}\|^2 + \|\mathbf{v}_{2,q}\|^2 = 1$. We then have:

$$\frac{1}{N} \mathbb{E} (\|\mathbf{v}\|^2) = \frac{1}{N} \sum_{q=1}^Q \mathbb{E} \left[\left(\|\mathbf{v}_{1,q}\|^2 - \|\mathbf{v}_{1,q}\|^4 \right) \sigma_n^2 \right] \quad (\text{A.22})$$

To determine (A.22), we need to know the transformations performed by the singular value decomposition on the input matrix \mathbf{A} to obtain $\mathbf{v}_{1,q}$ and σ_n^2 , i.e., we have to find an analytic expression of $\mathbf{v}_{1,q}$ and σ_n^2 . We know that:

$$\mathbf{A} = \mathbf{S}^H \mathbf{H}_B = \begin{bmatrix} z_1 & 0 & \dots & 0 & z_2 & 0 & \dots & 0 & \dots & z_U & 0 & \dots & 0 \\ 0 & z_{U+1} & \dots & 0 & 0 & z_{U+2} & \dots & 0 & \dots & 0 & z_{2U} & \dots & 0 \\ \vdots & & \ddots & \vdots & \vdots & & \ddots & \vdots & \dots & \vdots & & \ddots & \vdots \\ 0 & 0 & \dots & z_{(N-1)U+1} & 0 & 0 & \dots & z_{(N-1)U+2} & \dots & 0 & 0 & \dots & z_Q \end{bmatrix} \quad (\text{A.23})$$

where $\mathbf{A} \in \mathcal{C}^{N \times Q}$ and $z_i = z_{i,x} + jz_{i,y} \sim \mathcal{CN}(0, \frac{1}{U}) \sim \mathcal{N}(0, \frac{1}{2U}) + j\mathcal{N}(0, \frac{1}{2U})$. After singular value decomposition, we obtain:

$$\Sigma = \begin{bmatrix} \sigma_1 & 0 & \dots & 0 \\ 0 & \sigma_2 & \dots & 0 \\ \vdots & & \ddots & \vdots \\ 0 & 0 & \dots & \sigma_N \end{bmatrix} \quad (\text{A.24})$$

where $\sigma_n = \sqrt{\sum_{i=1}^U |z_{(n-1)U+i}|^2}$, $n = 1 \dots N$

$$\mathbf{V}_1 = \begin{bmatrix} v_1 & 0 & \dots & 0 \\ 0 & v_{U+1} & \dots & 0 \\ \vdots & & \ddots & \vdots \\ 0 & 0 & \dots & v_{(U-1)N+1} \\ v_2 & 0 & \dots & 0 \\ 0 & v_{U+2} & \dots & 0 \\ \vdots & & \ddots & \vdots \\ 0 & 0 & \dots & v_{(U-1)N+2} \\ \vdots & \vdots & & \vdots \\ v_U & 0 & \dots & 0 \\ 0 & v_{2U} & \dots & 0 \\ \vdots & & \ddots & \vdots \\ 0 & 0 & \dots & v_Q \end{bmatrix} \quad (\text{A.25})$$

where $v_i = \frac{z_i^*}{\sigma_k}$, $i = 1 \dots Q$, $k = 1 \dots N$ represents the column of \mathbf{V}_1 where v_i belongs. From that, we obtain:

$$\mathbb{E} [\sigma_n^2] = \mathbb{E} \left[\sum_{i=1}^U |z_{(n-1)U+i}|^2 \right] \quad (\text{A.26a})$$

$$= U \mathbb{E} \left[|z_{(n-1)U+i}|^2 \right] \quad (\text{A.26b})$$

$$= U \frac{1}{U} \quad (\text{A.26c})$$

$$= 1 \quad (\text{A.26d})$$

Without loss of generality, we compute $\mathbb{E} [\|v_1\|^2]$ and $\mathbb{E} [\|v_1\|^4]$ since all components of \mathbf{V}_1 are identically distributed:

$$\mathbb{E} [\|v_1\|^2] = \mathbb{E} \left[\left| \frac{z_1^*}{\sigma_1} \right|^2 \right] \quad (\text{A.27a})$$

$$= \mathbb{E} \left[\frac{|z_1|^2}{\sigma_1^2} \right] \quad (\text{A.27b})$$

$$= \mathbb{E} \left[\frac{|z_1|^2}{\sum_{i=1}^U |z_i|^2} \right] \quad (\text{A.27c})$$

$$= \mathbb{E} \left[\frac{|z_1|^2}{U |z_1|^2} \right] \quad (\text{A.27d})$$

$$= \frac{1}{U} \quad (\text{A.27e})$$

For the moment of order 4, we note that $\mathbb{E} [|z_i|^4] = \frac{2}{U^2}^{10}$.

$$\mathbb{E} [\|v_1\|^4] = \mathbb{E} \left[\left| \frac{z_1^*}{\sigma_1} \right|^4 \right] \quad (\text{A.28a})$$

$$= \mathbb{E} \left[\frac{|z_1|^4}{\sigma_1^4} \right] \quad (\text{A.28b})$$

$$= \mathbb{E} \left[\frac{|z_1|^4}{\left(\sum_{i=1}^U |z_i|^2 \right)^2} \right] \quad (\text{A.28c})$$

$$= \mathbb{E} \left[\frac{|z_1|^4}{\sum_{i=1}^U |z_i|^4 + 2 \sum_{i=1}^U \sum_{j<i} |z_i|^2 |z_j|^2} \right] \quad (\text{A.28d})$$

$$= \mathbb{E} \left[\frac{|z_1|^4}{U |z_1|^4 + 2 \frac{(U-1)U}{2} |z_1|^2 |z_j|^2} \right] \quad (\text{A.28e})$$

$$= \frac{\frac{2}{U^2}}{U \frac{2}{U^2} + 2 \frac{(U-1)U}{2} \frac{1}{U} \frac{1}{U}} \quad (\text{A.28f})$$

$$= \frac{\frac{2}{U^2}}{\frac{U+1}{U}} \quad (\text{A.28g})$$

$$= \frac{2}{U(U+1)} \quad (\text{A.28h})$$

The double sum on the denominator of (A.28d) contains $\frac{(U-1)U}{2}$ double products.

Finally, we can compute (A.22) as:

$$\frac{1}{N} \mathbb{E} (\|\mathbf{v}\|^2) = \frac{1}{N} \sum_{q=1}^Q \left[\left(\frac{1}{U} - \frac{2}{U(U+1)} \right) 1 \right] \quad (\text{A.29a})$$

$$= \frac{1}{N} Q \frac{U-1}{U(U+1)} \quad (\text{A.29b})$$

$$= \frac{U-1}{U+1} \quad (\text{A.29c})$$

which is the mean energy per AN received symbol when Eve implements a matched filter.

As previously mentioned, we omitted the weighting coefficient β . Without this coefficient, we have $\mathbb{E} [|\mathbf{w}|^2] = \mathbb{E} [|\mathbf{V}_2 \mathbf{w}'|^2] = \frac{U-1}{U}$. In the simulation, we assumed $\mathbb{E} [|\mathbf{w}|^2] = \frac{1}{U}$, such that the coefficient must correct (A.29c) by $\beta = \frac{1}{U-1}$.

With the correction taken into account, the final expression for the mean energy per AN received symbol when Eve implements a matched filter is given by:

$$\frac{1}{N} \mathbb{E} (\|\mathbf{v}\|^2) = \frac{1}{U+1} \quad (\text{A.30})$$

A.2.3 AN suppression

In this scenario, the received signal at Eve is given by:

$$\mathbf{y}_E^G = \sqrt{\alpha} \mathbf{S}^H |\mathbf{H}_B|^2 \mathbf{S} \mathbf{x} + \mathbf{S}^H \mathbf{H}_E^{-1} \mathbf{H}_B \mathbf{v}_E \quad (\text{A.31})$$

¹⁰see Appendix C

Data component

In what concerns the data component, the computation is straightforward since it is similar to (A.3). We then obtain $\mathbb{E}[|A_{1,n}|^2] = \alpha \frac{U+1}{U}$.

Additive white gaussian noise component

The noise term is:

$$\mathbb{E}[|\mathbf{A}_2|^2] = \mathbb{E}\left[\left|\mathbf{S}^H \mathbf{H}_B \mathbf{H}_E^{-1} \mathbf{v}_E\right|^2\right] \quad (\text{A.32a})$$

$$= \mathbb{E}\left[\left(\mathbf{S}^H \mathbf{H}_B \mathbf{H}_E^{-1} \mathbf{v}_E\right) \left(\mathbf{S}^H \mathbf{H}_B \mathbf{H}_E^{-1} \mathbf{v}_E\right)^H\right] \quad (\text{A.32b})$$

$$= \mathbb{E}\left[\mathbf{S}^H |\mathbf{H}_B|^2 |\mathbf{H}_E^{-1}|^2 |\mathbf{v}_E|^2 \mathbf{S}\right] \quad (\text{A.32c})$$

$$\mathbb{E}[|A_{2,n}|^2] = \frac{1}{U} \mathbb{E}\left[\sum_{i=0}^{U-1} |h_{E,n+iN}^{-1}|^2 |h_{B,n+iN}|^2 |v_{E,n+iN}|^2\right] \quad (\text{A.32d})$$

$$= \sigma_{V,E}^2 \mathbb{E}\left[|h_{E,n+iN}^{-1}|^2\right] = \sigma_{V,E}^2 \mathbb{E}\left[\frac{1}{|h_{E,n+iN}|^2}\right] \quad (\text{A.32e})$$

The issue that arises in (A.32e) is that the variable $X = \frac{1}{|h_{E,n+iN}|^2}$ follows an inverse chi-square distribution of $\nu = 2$ degrees of freedom. The expected value of such a distribution is given by:

$$\mathbb{E}[X] = \frac{1}{\nu - 2} = +\infty \quad (\text{A.33})$$

Eq. (A.33) suggests that the expected value of the energy of the noise component is infinite which implies that the ergodic SINR at Eve tends to zero and that the ergodic SR of the communication tends to the ergodic capacity of Bob. However, this is only the case when $|h_{E,n+iN}|^2 = 0$, i.e. when a subcarrier of Eve's channel has a zero gain. From (A.32), we clearly understand that this decoding structure will amplify the noise component which is not optimal, as already anticipated from section 4.1.2.3. However, we can compute the probability p that our RV X is bigger than a certain threshold t , i.e., we can compute the upper-bound value of the SR with a given probability. The probability density function (PDF) of X has the form:

$$f_X(x) = \frac{2^{-\nu/2}}{\Gamma(\nu/2)} x^{-\nu/2-1} e^{-\frac{1}{2x}} \quad (\text{A.34})$$

where $\Gamma(a) = (a-1)! = \int_0^\infty z^{a-1} e^{-z} dz$ is the Gamma function of the integer a . The probability that our RV X is bigger than t is given by:

$$\begin{aligned} Pr(t < X) &= \int_t^{+\infty} f_X(x) dx = p \\ \Leftrightarrow p &= \int_t^{+\infty} \frac{2^{-1}}{\Gamma(1)} x^{-2} e^{-\frac{1}{2x}} dx \\ \Leftrightarrow p &= \int_{1/t}^0 e^{-u/2} du \\ \Leftrightarrow p &= 1 - e^{-\frac{1}{2t}} \\ \Leftrightarrow t &= \frac{-2}{\ln(1-p)} \end{aligned} \quad (\text{A.35})$$

This relation is plotted in fig.A.1 where we see that we have for example a probability of $p = 5\%$ that our decoding structure will amplify the noise component by a factor $t = 27$.

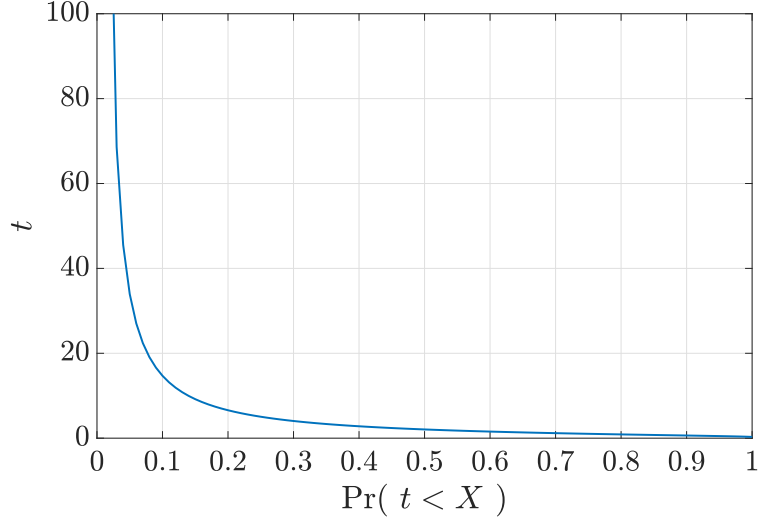


Figure A.1: CDF of the inverse chi-square distribution of $\nu = 2$ degrees of freedom.

A.2.4 LMMSE

As a recall, the LMMSE equalizer \mathbf{G} needs to satisfy the orthogonality principle. In doing so, we have:

$$\mathbb{E} [(\hat{\mathbf{x}}_E - \mathbf{x})\mathbf{y}_E^H] = \mathbf{0} \quad (\text{A.36a})$$

$$\Leftrightarrow \mathbb{E} [(\mathbf{G}\mathbf{Y}_E - \mathbf{x})\mathbf{y}_E^H] = \mathbf{0} \quad (\text{A.36b})$$

$$\Leftrightarrow \mathbb{E} [\mathbf{G}\mathbf{Y}_E\mathbf{y}_E^H] = \mathbb{E} [\mathbf{x}\mathbf{y}_E^H] \quad (\text{A.36c})$$

$$\Leftrightarrow \mathbf{G} = \mathbb{E} [\mathbf{x}\mathbf{y}_E^H] \left(\mathbb{E} [\mathbf{Y}_E\mathbf{y}_E^H] \right)^{-1} \quad (\text{A.36d})$$

$$\Leftrightarrow \mathbf{G} = \mathbb{E} \left[\mathbf{x} \left(\sqrt{\alpha}\Gamma_E\mathbf{x} + \sqrt{1-\alpha}\mathbf{H}_E\mathbf{w} + \mathbf{v}_E \right)^H \right] \left(\mathbb{E} \left[\left(\sqrt{\alpha}\Gamma_E\mathbf{x} + \sqrt{1-\alpha}\mathbf{H}_E\mathbf{w} + \mathbf{v}_E \right) \left(\sqrt{\alpha}\Gamma_E\mathbf{x} + \sqrt{1-\alpha}\mathbf{H}_E\mathbf{w} + \mathbf{v}_E \right)^H \right] \right)^{-1} \quad (\text{A.36e})$$

$$\Leftrightarrow \mathbf{G} = \left(\sqrt{\alpha}\mathbb{E} [\mathbf{x}\mathbf{x}^H\Gamma_E^H] + \sqrt{1-\alpha}\mathbb{E} [\mathbf{x}\mathbf{w}^H\mathbf{H}_E^H] + \mathbb{E} [\mathbf{x}\mathbf{v}_E^H] \right) \left(\mathbb{E} [\alpha\Gamma_E\Gamma_E^H\mathbf{x}\mathbf{x}^H + (1-\alpha)\mathbf{H}_E\mathbf{w}\mathbf{w}^H\mathbf{H}_E^H + \mathbf{v}_E\mathbf{v}_E^H] \right)^{-1} \quad (\text{A.36f})$$

$$\Leftrightarrow \mathbf{G} = \sqrt{\alpha}\sigma_X^2\Gamma_E^H \left(\alpha\sigma_X^2\Gamma_E\Gamma_E^H + (1-\alpha)|\mathbf{H}_E|^2\sigma_{AN}^2 + \sigma_{VE}^2\mathbf{I}_N \right)^{-1} \quad (\text{A.36g})$$

B Optimal amount of AN to inject derivation

B.1 Despredding at Eve

As a recall, the SINR at Bob and Eve are respectively given by:

$$\begin{aligned}\mathbb{E}[\gamma_{B,n}] &= \frac{\alpha(U+1)}{U\sigma_{V,B}^2} \\ \mathbb{E}[\gamma_{E,n}] &= \frac{\alpha}{U(\sigma_{V,E}^2 + (1-\alpha)\sigma_{AN}^2)}\end{aligned}\tag{B.1}$$

The SR becomes:

$$C_s = \log_2 \left(1 + \frac{\alpha(U+1)}{U\sigma_{V,B}^2} \right) - \log_2 \left(1 + \frac{\alpha}{U(\sigma_{V,E}^2 + (1-\alpha)\sigma_{AN}^2)} \right)\tag{B.2a}$$

$$\Leftrightarrow C_s = \log_2 \left(\frac{\alpha(U+1) + U\sigma_{V,B}^2}{U\sigma_{V,B}^2} \right) - \log_2 \left(\frac{\alpha + U\sigma_{V,E}^2 + (1-\alpha)U\sigma_{AN}^2}{U\sigma_{V,E}^2 + (1-\alpha)U\sigma_{AN}^2} \right)\tag{B.2b}$$

Remembering that $U\sigma_{AN}^2 = 1$, we obtain:

$$C_s = \log_2 \left(\frac{U\sigma_{V,B}^2 + \alpha(U+1)}{U\sigma_{V,B}^2} \cdot \frac{U\sigma_{V,E}^2 + 1 - \alpha}{U\sigma_{V,E}^2 + 1} \right)\tag{B.3a}$$

$$\Leftrightarrow C_s = \log_2 \left(\frac{-\alpha^2(U+1) + \alpha[(U+1)U\sigma_{V,E}^2 - U\sigma_{V,B}^2 + (U+1)] + U\sigma_{V,B}^2(U\sigma_{V,E}^2 + 1)}{U\sigma_{V,B}^2(U\sigma_{V,E}^2 + 1)} \right)\tag{B.3b}$$

If we introduce $T_1 = -(U+1)$, and $T_2 = (U+1)U\sigma_{V,E}^2 - U\sigma_{V,B}^2 + (U+1)$ we come back to (32).

B.2 Matched filtering at Eve

As a recall, the SINR at Bob and Eve are respectively given by:

$$\begin{aligned}\mathbb{E}[\gamma_{B,n}] &= \frac{\alpha(U+1)}{U\sigma_{V,B}^2} \\ \mathbb{E}[\gamma_{E,n}] &= \frac{\alpha \frac{U+3}{U}}{\sigma_{V,E}^2 + \frac{1-\alpha}{U+1}}\end{aligned}\tag{B.4}$$

If we multiply the SINR at Eve by $\frac{U+1}{U+3}$, the SR becomes:

$$C_s = \log_2 \left(1 + \frac{\alpha(U+1)}{U\sigma_{V,B}^2} \right) - \log_2 \left(1 + \frac{\alpha \frac{U+1}{U}}{\frac{U+1}{U+3}\sigma_{V,E}^2 + \frac{1-\alpha}{U+3}} \right)\tag{B.5a}$$

$$\Leftrightarrow C_s = \log_2 \left(\frac{1 + \frac{\alpha(U+1)}{U\sigma_{V,B}^2}}{1 + \frac{\alpha(U+1)(U+3)}{U[(U+1)\sigma_{V,E}^2 + (1-\alpha)]}} \right)\tag{B.5b}$$

$$\Leftrightarrow C_s = \log_2 \left(\frac{U\sigma_{V,B}^2 + \alpha(U+1)}{\sigma_{V,B}^2} \cdot \frac{(U+1)\sigma_{V,E}^2 + (1-\alpha)}{U(U+1)\sigma_{V,E}^2 + U(1-\alpha) + \alpha(U+1)(U+3)} \right)\tag{B.5c}$$

$$\Leftrightarrow C_s = \log_2 \left(\frac{-\alpha^2(U+1) + \alpha[(U+1)^2\sigma_{V,E}^2 + (U+1) - U\sigma_{V,B}^2] + [U(U+1)\sigma_{V,B}^2\sigma_{V,E}^2 + U\sigma_{V,B}^2]}{\alpha[(U+1)(U+3)\sigma_{V,B}^2 - U\sigma_{V,B}^2] + [U(U+1)\sigma_{V,B}^2\sigma_{V,E}^2 + U\sigma_{V,B}^2]} \right)\tag{B.5d}$$

If we introduce: $T_1 = U+1$, $T_2 = (U+1)^2\sigma_{V,E}^2 + (U+1) - U\sigma_{V,B}^2$, $T_3 = U(U+1)\sigma_{V,B}^2\sigma_{V,E}^2 + U\sigma_{V,B}^2$, and $T_4 = (U+1)(U+3)\sigma_{V,B}^2 - U\sigma_{V,B}^2$, we come back to (34).

C Momentum computation of complex-valued random normal variables

C.1 Real-valued random normal variable

For real-valued random variable, the moment-generating function is an alternative specification of its probability distribution. In particular, it allows to compute the moments of the probability distribution as:

$$m_n = \mathbb{E}[X^n] = M_X^{(n)}(0) = \left. \frac{d^n M_X}{dt^n} \right|_{t=0} \quad (\text{C.1})$$

For a real normal random variable $\mathcal{N}(\mu, \sigma^2)$, the moment-generating function is given by:

$$M_X = e^{t\mu + \frac{1}{2}\sigma^2 t^2} \quad (\text{C.2})$$

From that, we have:

$$\begin{aligned} \mathbb{E}[|X|^2] &= \sigma^2 + \mu^2 \\ \mathbb{E}[|X|^4] &= 3(\sigma^2)^2 + 6\sigma^2\mu^2 + \mu^4 \end{aligned} \quad (\text{C.3})$$

C.2 Complex-valued random normal variable

A complex normal random variable is defined as $Z = X + iY$ where $X \sim \mathcal{N}(\mu_x, \sigma_x^2)$ and $Y \sim \mathcal{N}(\mu_y, \sigma_y^2)$. We also have:

$$\begin{aligned} |Z|^2 &= X^2 + Y^2 \\ |Z|^4 &= X^4 + 2X^2Y^2 + Y^4 \end{aligned} \quad (\text{C.4})$$

Since X and Y are independent and taking into account eq.C.3, the moments of Z are easy to compute:

$$\begin{aligned} \mathbb{E}[|Z|^2] &= \sigma_x^2 + \mu_x^2 + \sigma_y^2 + \mu_y^2 \\ \mathbb{E}[|Z|^4] &= 3(\sigma_x^2)^2 + 6\sigma_x^2\mu_x^2 + \mu_x^4 + 2[(\sigma_x^2 + \mu_x^2)(\sigma_y^2 + \mu_y^2)] + 3(\sigma_y^2)^2 + 6\sigma_y^2\mu_y^2 + \mu_y^4 \end{aligned} \quad (\text{C.5})$$